PREPRINT: This manuscript is a preprint submitted to EarthArXiv. This version 2 reflects the revisions made in response to a first round of peer-review by the GSA Books volume “Jurassic–Paleogene tectonic evolution of the North American Cordillera” of the Geological Society of America (resubmitted to the editors on 2025/01/01).

Tomotectonics of Cordilleran North America since Jurassic times: double-sided subduction, archipelago collisions, and Baja-BC translation

Karin Sigloch[1] & Mitchell G. Mihalynuk[2]

1) Université Côte d’Azur, Observatoire Côte d’Azur, CNRS, IRD. Géoazur, Sophia Antipolis, France. sigloch@geoazur.unice.fr
2) British Columbia Geological Survey. Ministry of Energy, Mines and Low Carbon Innovation British Columbia. Victoria, Canada. Mitch.Mihalynuk@gov.bc.ca

Figure 1

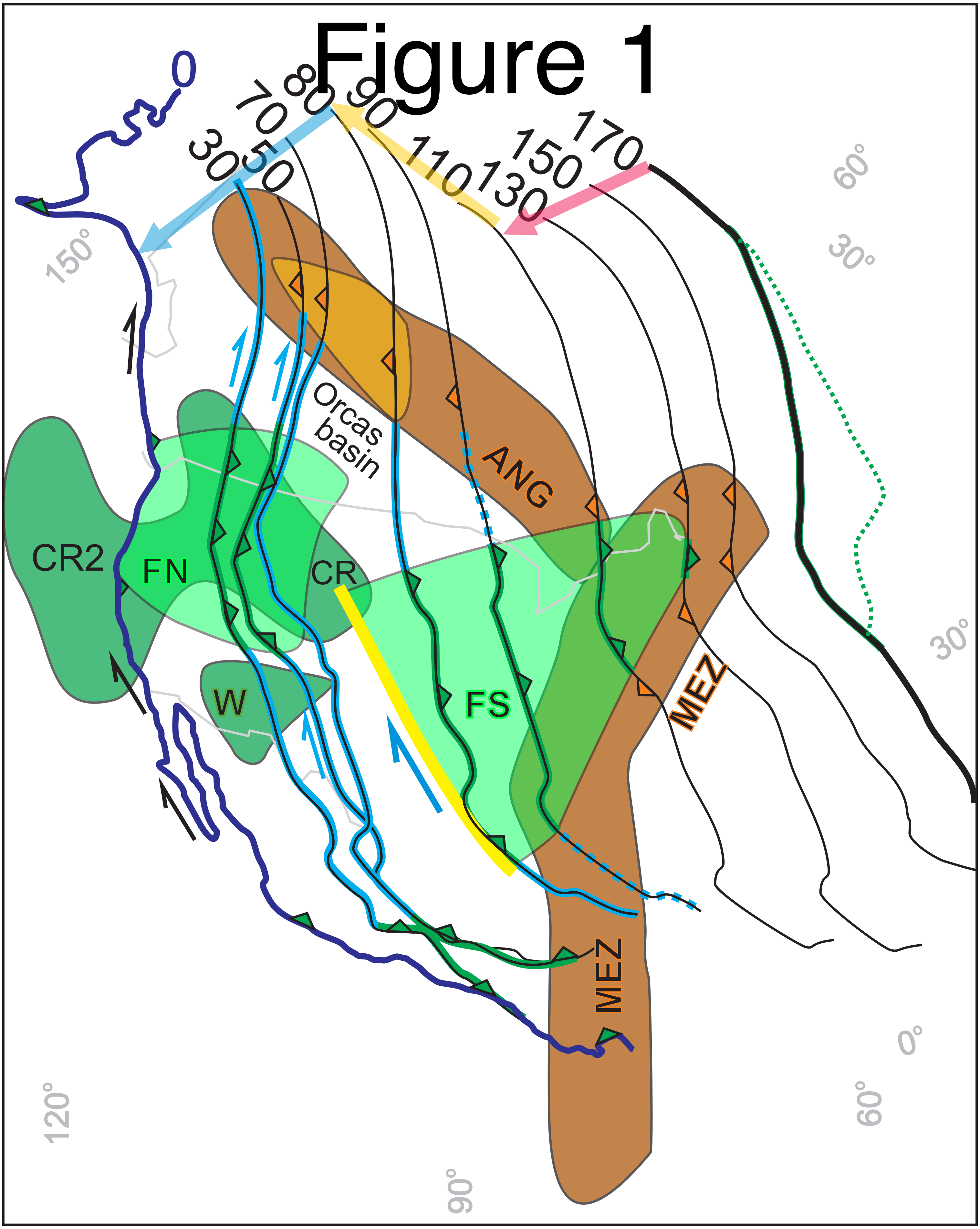
0
30
50
70
80
90
110
130
150
170
Orcas basin
ANG
MEZ
MEZ
CR2
FN
CR
W
FS
150°
60°
30°
30°
0°
120°
90°
60°

Figure 2

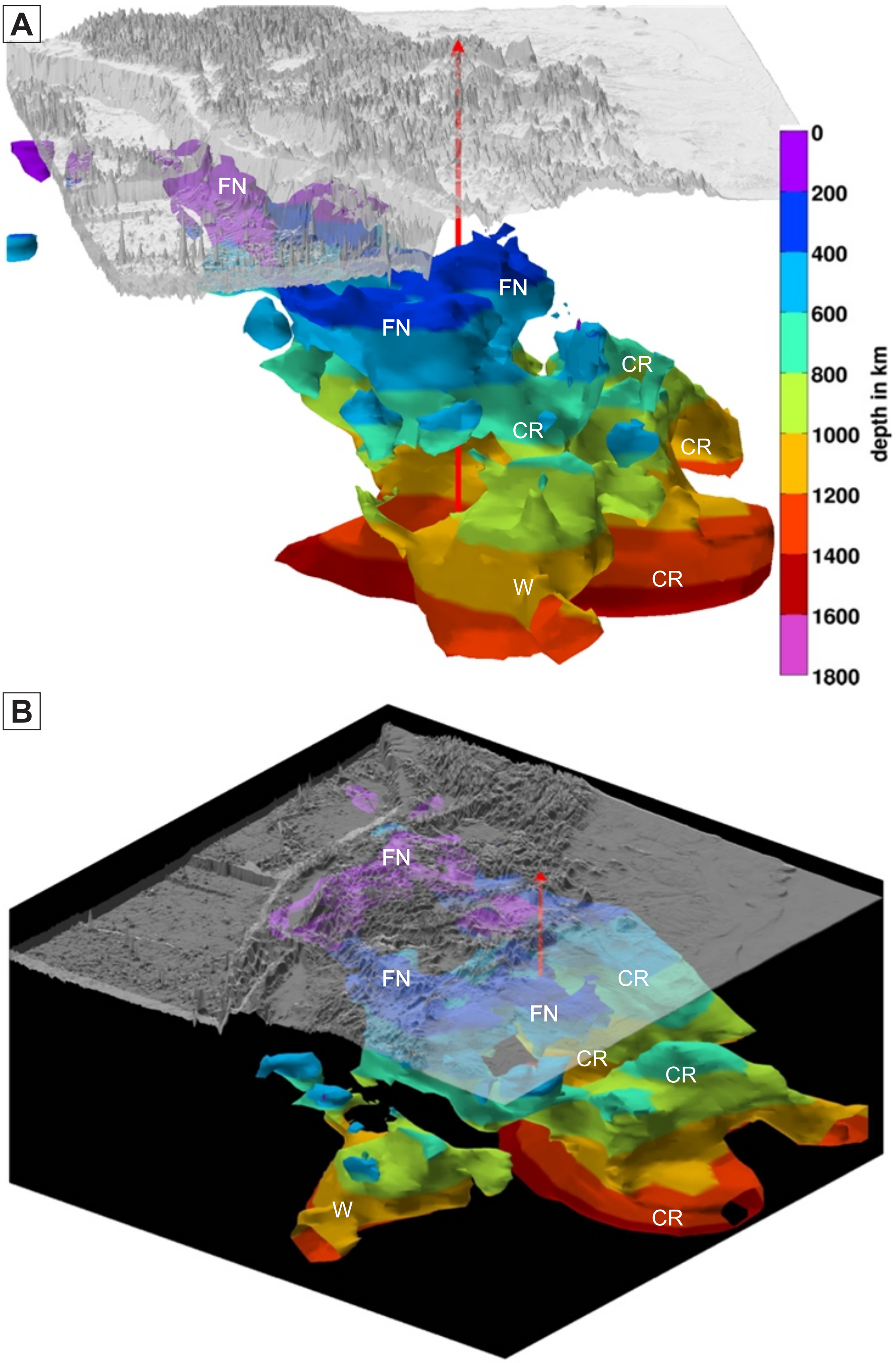
A
FN
FN
FN
CR
CR
CR
W
CR
0
200
400
600
800
1000
1200
1400
1600
1800
depth in km
B
FN
FN
CR
FN
CR
CR
W
CR

Figure 3

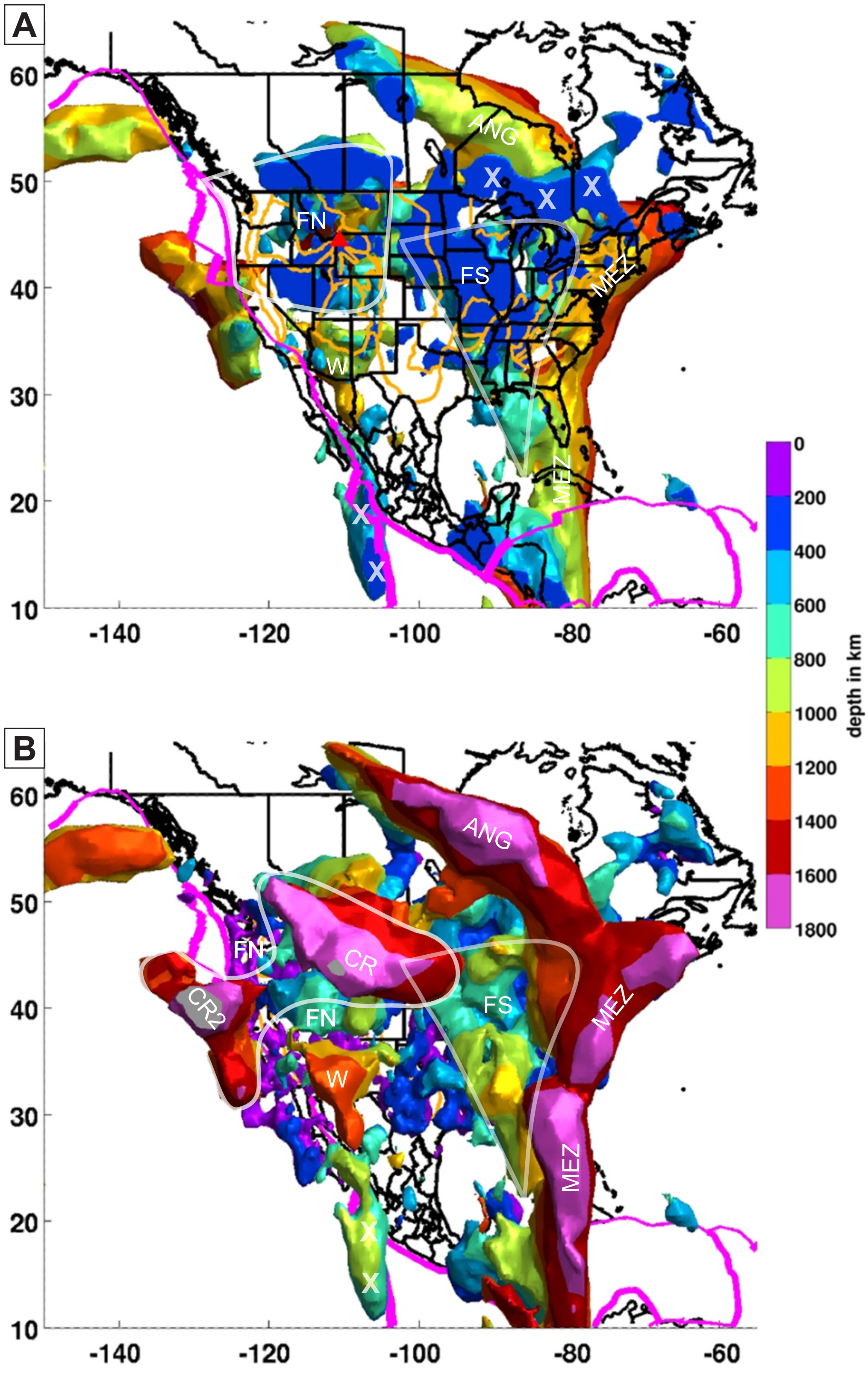
A
B
ANG
FN
FS
MEZ
W
X
CR
CR2
60
50
40
30
20
10
-140
-120
-100
-80
-60
0
200
400
600
800
1000
1200
1400
1600
1800
depth in km

Figure 4

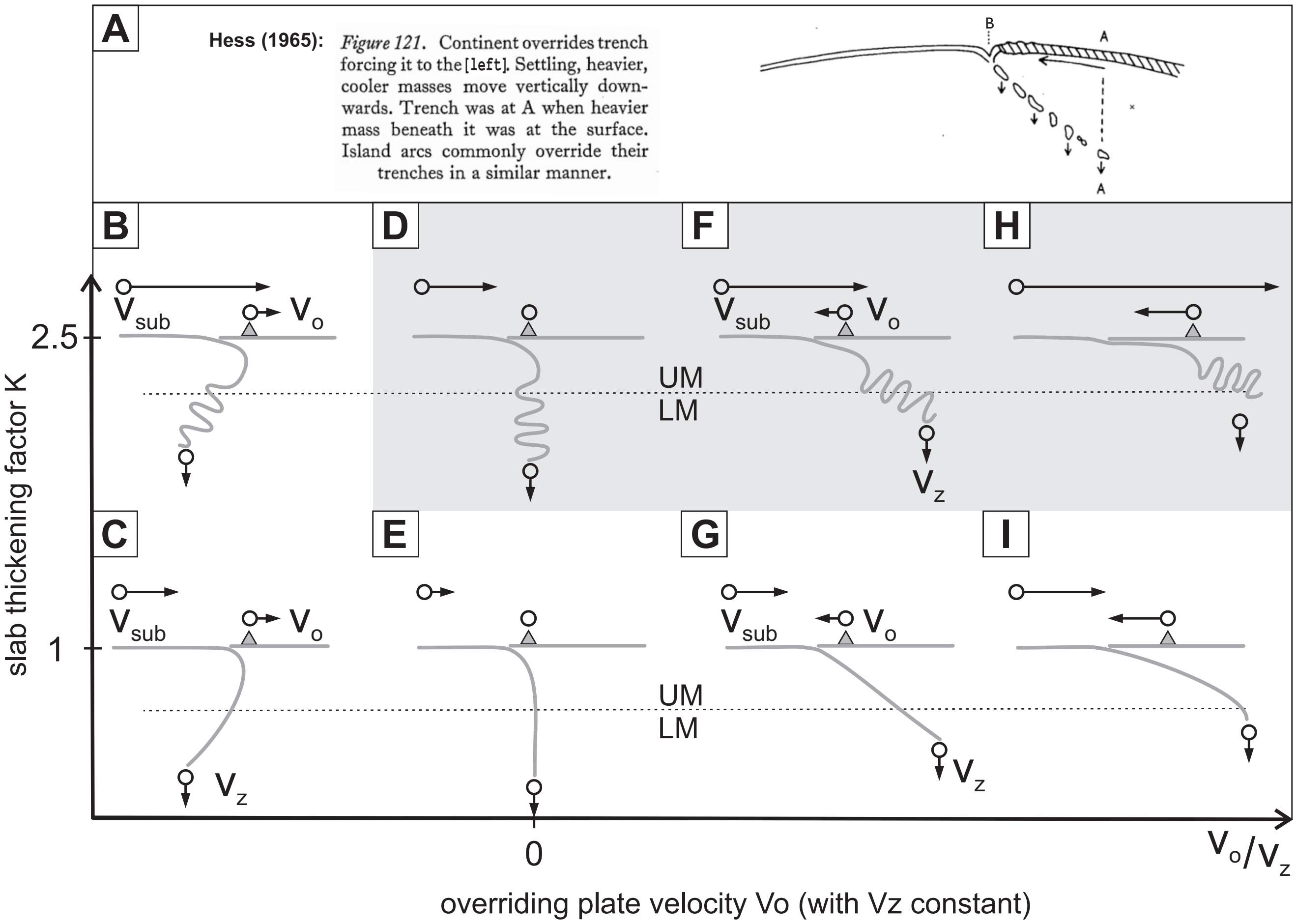

A
Hess (1965):
Figure 121. Continent overrides trench forcing it to the [left]. Settling, heavier, cooler masses move vertically downwards. Trench was at A when heavier mass beneath it was at the surface. Island arcs commonly override their trenches in a similar manner.
B
A
A
B
D
F
H
C
E
G
I
V_{sub}
V_o
V_z
UM
LM
2.5
1
0
slab thickening factor K
V_o/V_z
overriding plate velocity Vo (with Vz constant)

Figure 5

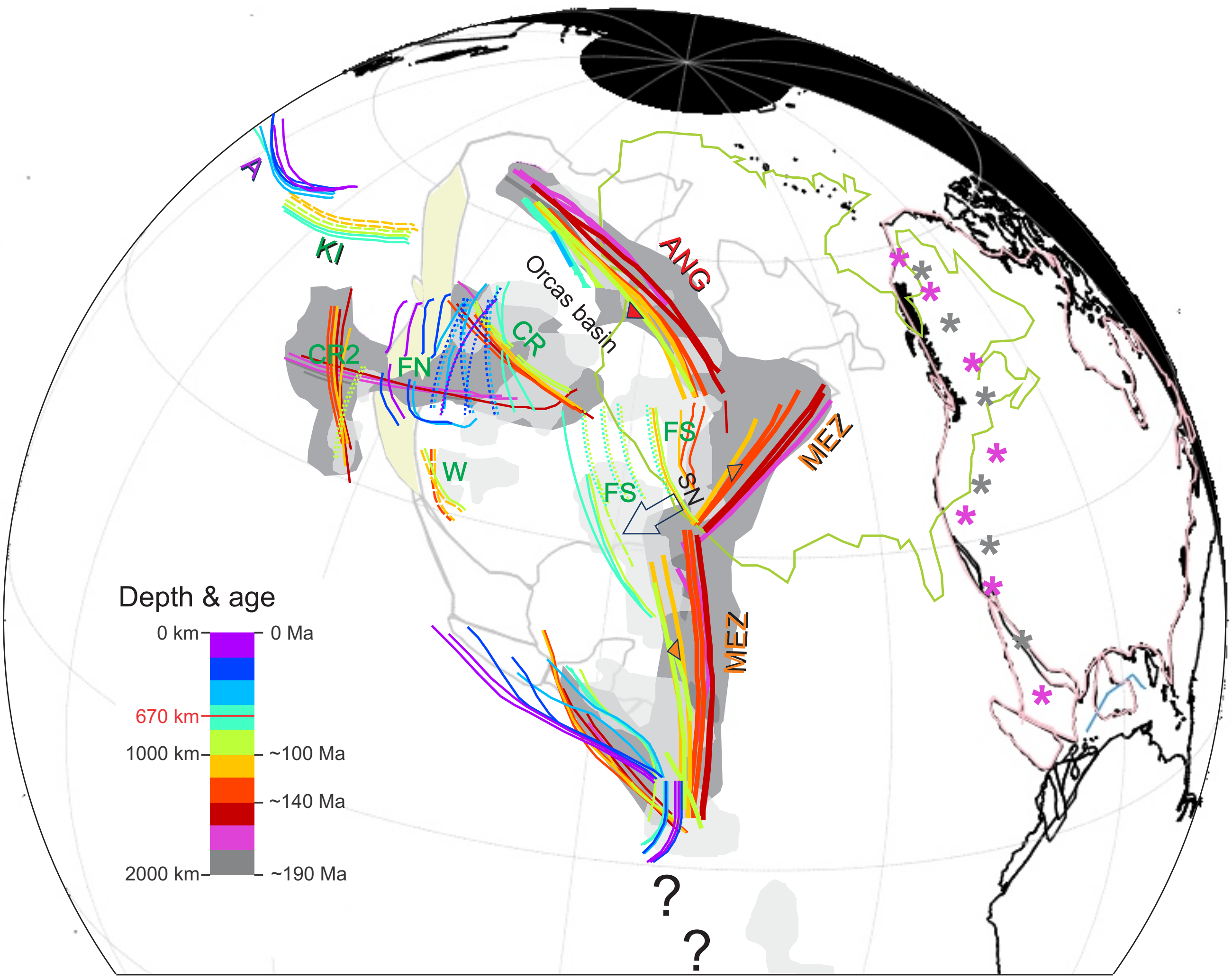

A
KI
CR2
FN
CR
Orcas basin
ANG
FS
W
FS
SN
MEZ
MEZ
Depth & age
0 km
0 Ma
670 km
1000 km
~100 Ma
~140 Ma
2000 km
~190 Ma
?
?

Figure 6

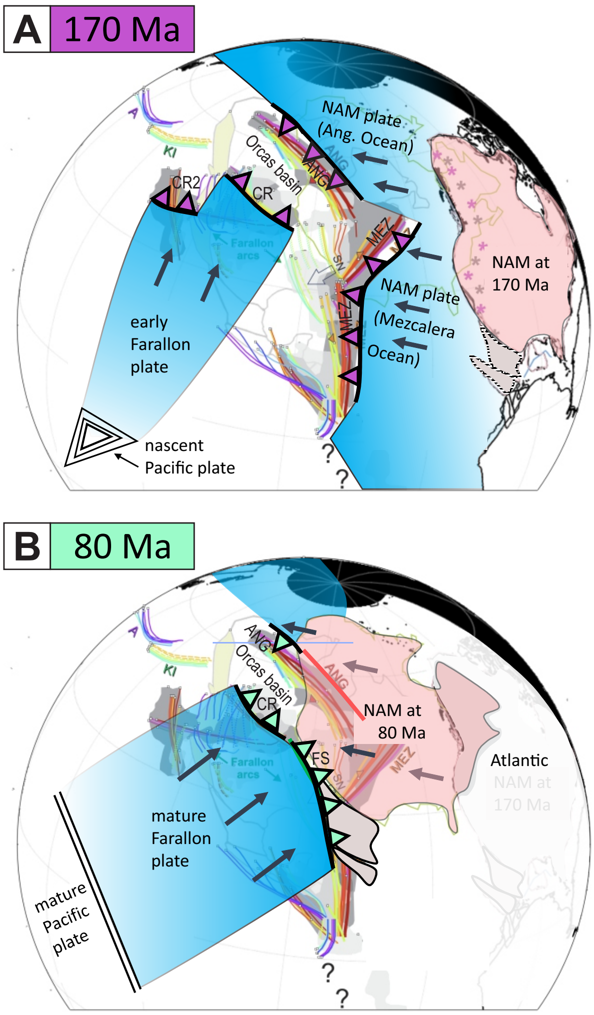

A
170 Ma
NAM plate
(Ang. Ocean)
Orcas basin
ANG
CR2
CR
MEZ
NAM plate
(Mezcalera
Ocean)
NAM at
170 Ma
early
Farallon
plate
nascent
Pacific plate
B
80 Ma
ANG
Orcas basin
CR
NAM at
80 Ma
FS
MEZ
Atlantic
NAM at
170 Ma
mature
Farallon
plate
mature
Pacific
plate

Figure 7

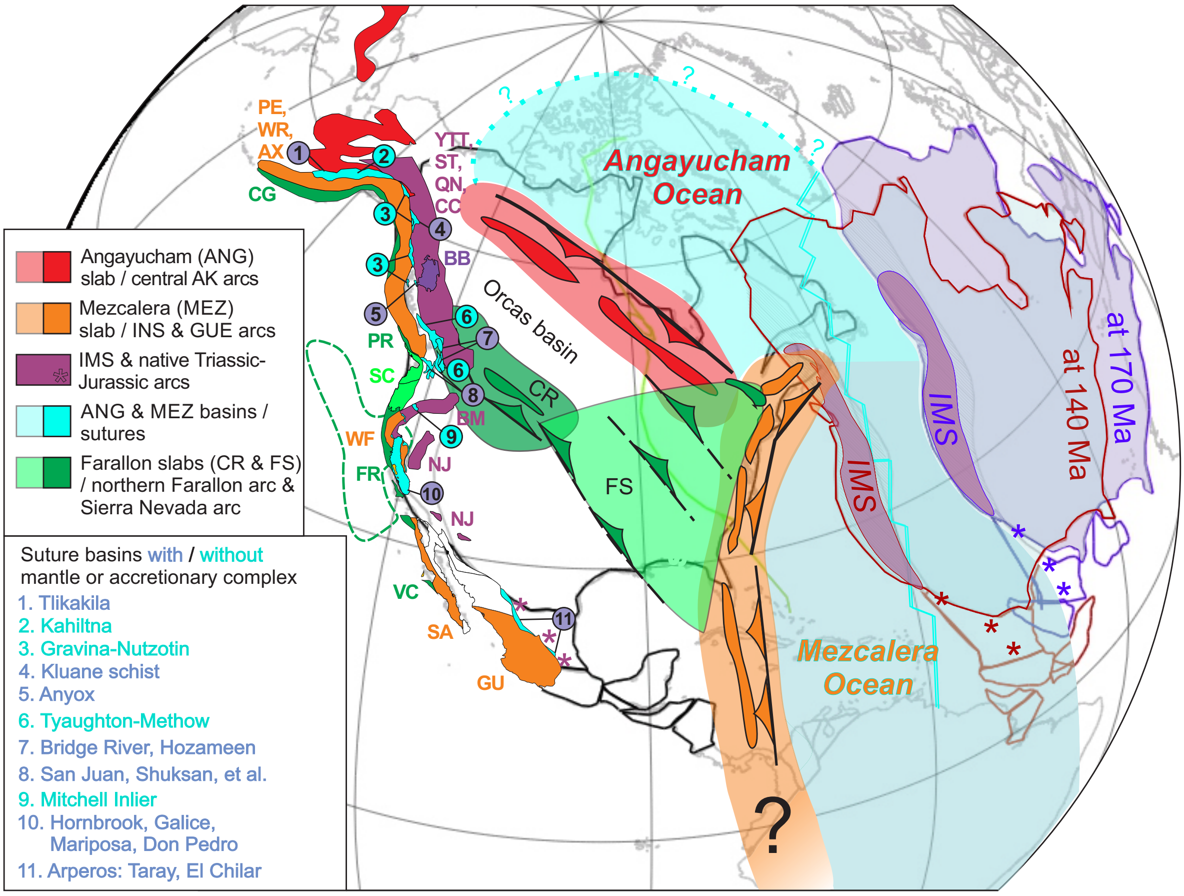

Angayucham Ocean
Mezcalera Ocean
Orcas basin
CR
FS
IMS
IMS
at 140 Ma
at 170 Ma
PE, WR, AX
CG
YTT, ST, QN, CC
BB
PR
SC
WF
FR
BM
NJ
NJ
VC
SA
GU
?
Angayucham (ANG) slab / central AK arcs
Mezcalera (MEZ) slab / INS & GUE arcs
IMS & native Triassic-Jurassic arcs
ANG & MEZ basins / sutures
Farallon slabs (CR & FS) / northern Farallon arc & Sierra Nevada arc
Suture basins with / without mantle or accretionary complex
1. Tlikakila
2. Kahiltna
3. Gravina-Nutzotin
4. Kluane schist
5. Anyox
6. Tyaughton-Methow
7. Bridge River, Hozameen
8. San Juan, Shuksan, et al.
9. Mitchell Inlier
10. Hornbrook, Galice, Mariposa, Don Pedro
11. Arperos: Taray, El Chilar

Figure 8

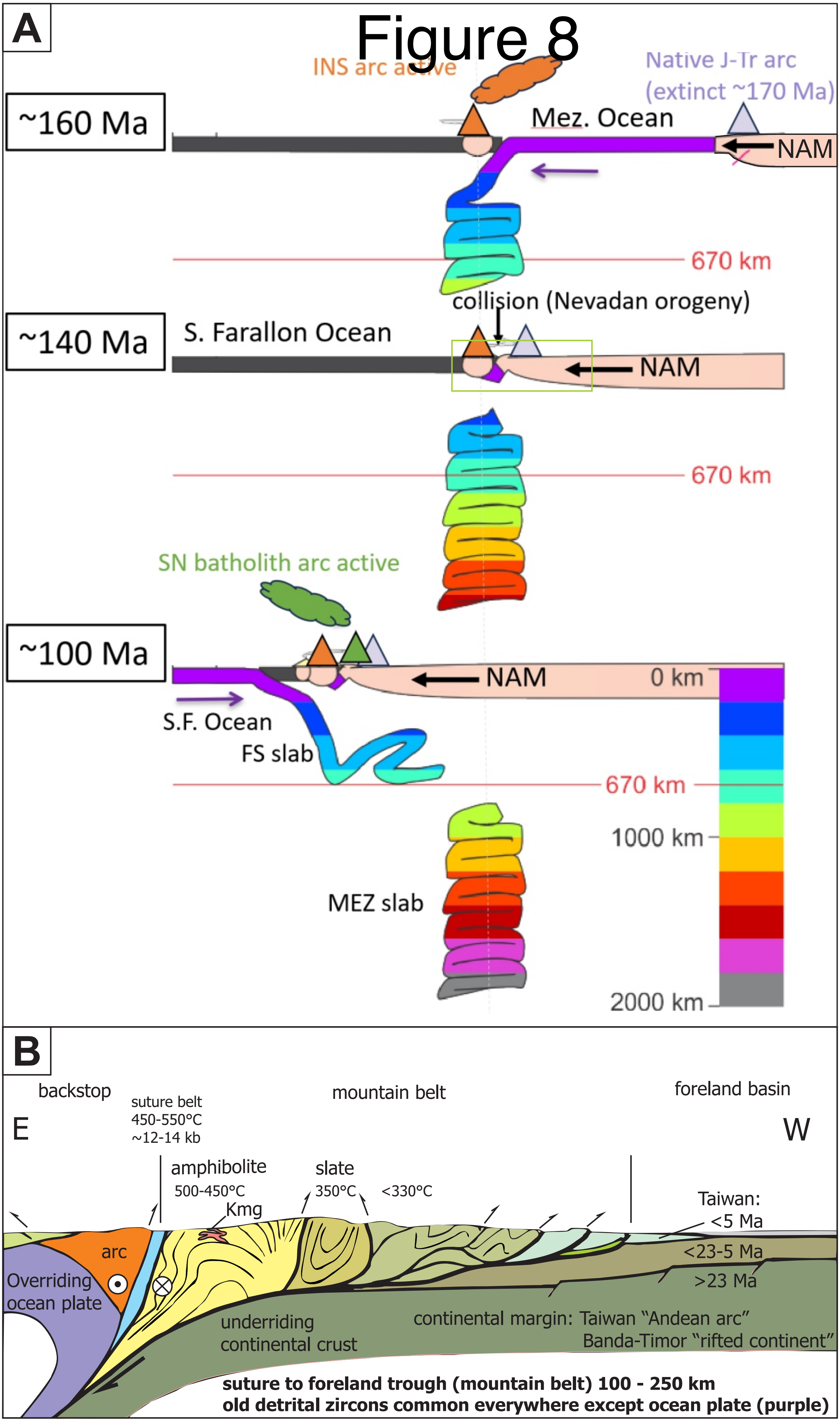

A
INS arc active
Native J-Tr arc
(extinct ~170 Ma)
~160 Ma
Mez. Ocean
NAM
670 km
collision (Nevadan orogeny)
~140 Ma
S. Farallon Ocean
NAM
670 km
SN batholith arc active
~100 Ma
NAM
0 km
S.F. Ocean
FS slab
670 km
1000 km
MEZ slab
2000 km
B
backstop
suture belt
450-550°C
~12-14 kb
mountain belt
foreland basin
E
W
amphibolite
500-450°C
Kmg
slate
350°C
<330°C
Taiwan:
<5 Ma
<23-5 Ma
>23 Ma
arc
Overriding
ocean plate
underriding
continental crust
continental margin: Taiwan "Andean arc"
Banda-Timor "rifted continent"
suture to foreland trough (mountain belt) 100 - 250 km
old detrital zircons common everywhere except ocean plate (purple)

Figure 9

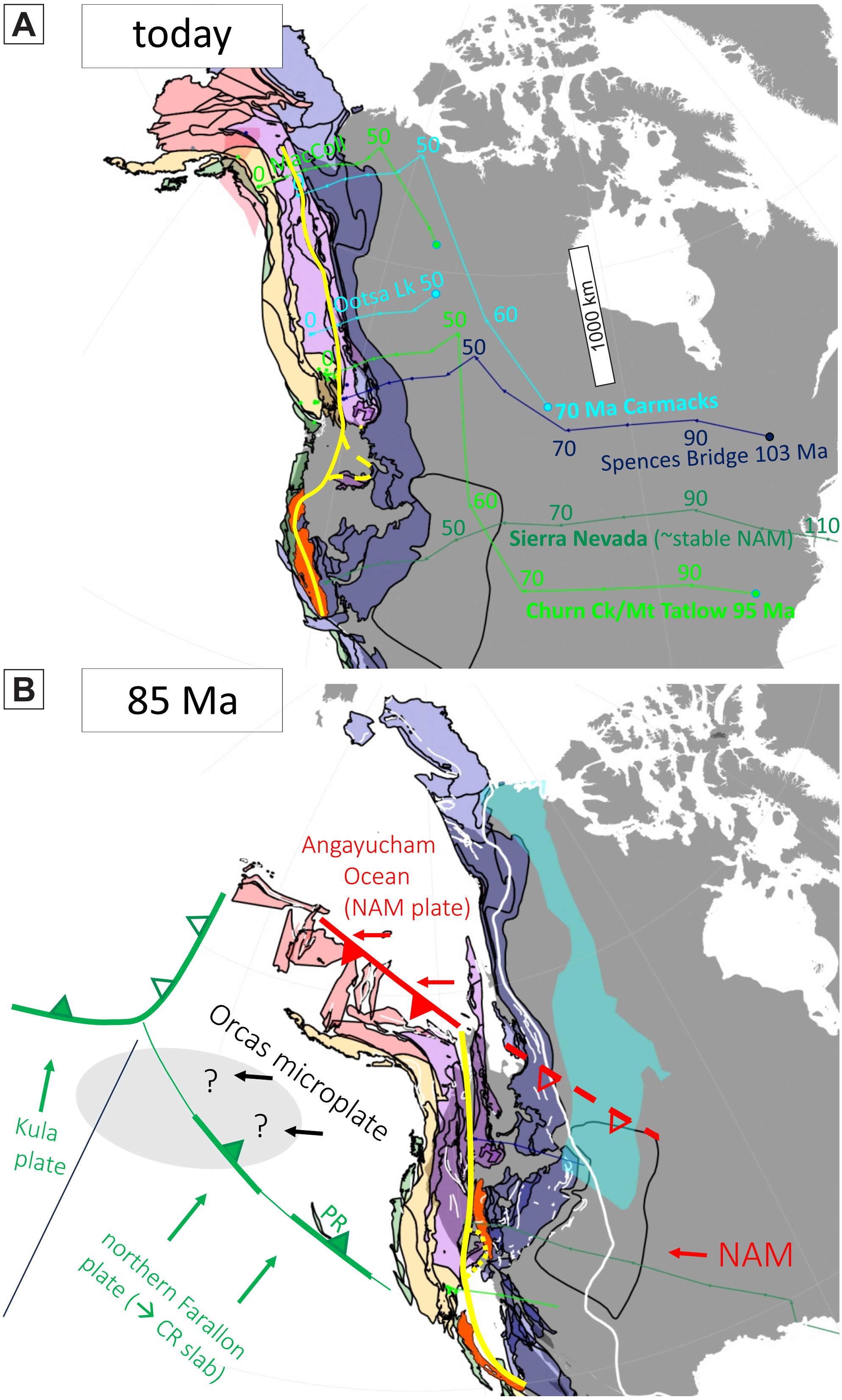
A
today
0 MacColl 50
50
Dotsa Lk 50
0
50
60
0
50
1000 km
70 Ma Carmacks
70
90
Spences Bridge 103 Ma
60
70
90
110
50
Sierra Nevada (~stable NAM)
70
90
Churn Ck/Mt Tatlow 95 Ma
B
85 Ma
Angayucham
Ocean
(NAM plate)
Orcas microplate
?
?
Kula
plate
PR
northern Farallon
plate (→ CR slab)
NAM

Figure captions

Figure 1. Roadmap figure for this study: the superposition of subducted lithosphere (slabs) in the mantle with continental drift, reconstructed with respect to the mantle. Coloured polygons show outlines of major slabs under North America from teleseismic P-wave tomography (Sigloch 2011). Slabs inferred to have been deposited by westward subduction are coloured in orange, those generated by eastward (Farallon) subduction in green. Darker colour shades are applied to lower-mantle slabs (MEZ, ANG and CR/CR2/W; light shades to shallower slabs: FS (400-1000 km deep), FN (0-700 km), and to the shallow western end of ANG. Superimposed are time snapshots tracking the westward migrating margin of North America, reconstructed in a mantle reference frame, which is constrained between 0-120 Ma by moving hotspots (Dubrovine et al., 2012) and 120-170 Ma by true polar wander-corrected paleomagnetic data (Torsvik et al., 2019). Colored arrows connecting the northern end points of the paleo-coastlines highlight three distinct episodes of absolute plate motion.
If the slabs sank vertically in place then a continental margin overlying a slab indicates a continent-arc interaction – because a slab constrains a paleo-subduction zone, which must have hosted a paleo-arc. Symbols on the paleo-margins indicate the nature of the tectonic regime along the margin, as inferable from the tomotectonic principles developed in the text. Orange barbs: NAM-beneath-arc collision (westward subducting slab located underneath). Green barbs: subduction beneath NAM (eastward subduction), with arc built on NAM. Light blue lines and arrows: transform boundary along the margin (no slab underneath). Black line: (quasi-)passive continental margin (no slab underneath, and no pre-existing plate boundary along the margin). Yellow line traces the sharp western edge of FS slab, associated with a sudden transition from eastward subduction to transform margin ~80 Ma. The starting point of our inference is ~170 Ma, the time when North America separated from Pangaea, and when absolute paleo-positioning in plate reconstructions becomes reasonably reliable.
Slab abbreviations: MEZ – Mezcalera, ANG – Angayucham, CR & CR2 – Cascadia Root, FN – Farallon North, FS – Farallon South. W is a non-interpretive slab name.

Figure 2. Mantle tomography: 3-D isosurface rendering of seismically fast anomalies imaged under the western U.S.A., from the surface to ~1800 km depth, in the teleseismic P-wave tomography model of Sigloch (2011). The isosurface rendering threshold is dVp/Vp>0.25%. Color signals depth and changes in increments of 200 km. This structure represents subducted oceanic lithosphere (slab) of the former Farallon plate, dipping eastward down from beneath the Cascades (Juan de Fuca) trench. Surface topography of the North American Cordillera and the Pacific basin are overlain in translucent gray, with strong vertical exaggeration. Yellowstone (red triangle) and its vertical downward continuation are shown for visual reference. Seismically slow anomalies are not rendered (e.g., Yellowstone plume). Shallow fast anomalies representing the thick continental lithosphere of NAM are masked out as they would block the 3-D view on the slabscape. Panels A and B present alternative view angles on the same scene, comprising the FN and CR slabs of Figure 1 (subdivided at ~600 km depth, where structural breaks are visible especially in panel B). Slab W is also visible in the foreground. Deep CR2 slab under the Pacific is not rendered.

Figure 3. Three-dimensional isosurface rendering of all seismically fast P-wave anomalies (subducted slabs) in the upper and lower mantle beneath North America. Tomography model, rendering threshold and color scheme as in Figure 2. (A) Top-down view of fast structure below 400 km (in order to exclude the overlying lithosphere, which is fast but does not represent slab). Strictly speaking, the view is from ~390 km down due to slight interpolation smoothing of the contouring algorithm, explaining why the shallowest anomalies appear in dark blue, as part of the 200-400 km layer. (B) Inside-out view of all fast structure from the surface down, with the deepest structure (slab walls MEZ, ANG, CR/CR2) emerging

to the foreground. Imaging limitations include artifacts, especially near the margins of the regional dataset: resolution lost into the ocean basins and north of 55°. Two downward smearing artifacts are labeled with white x's and are not interpreted.

Figure 4. (A) The tomotectonic null hypothesis of vertical slab sinking, as envisioned by the very first cartoon of subduction to be published, by Harry Hess in 1965. Motions are drawn in a mantle reference frame, with the overriding plate moving laterally but not the subducting plate. (B)-(I) Range of possible slab geometries predicted for when oceanic lithosphere sinks vertically after entering the trench, as a function of the parameters v_o, the velocity of the overriding plate (or arc) on the x-axis, and of K, a measure for the vigor of subduction, on the y-axis. Dashed lines represent the viscosity discontinuity between upper mantle (UM) and lower mantle (LM), where the mantle becomes 1-2 orders of magnitude more viscous, resisting further slab sinking. Motions are drawn relative to the mantle, and velocity arrows are drawn to scale relative to each other. v_z, the slab sinking velocity in the lower mantle, is kept fixed in all panels (a typical value being 10 mm/year). Kinematic ratio $K = v_{sub}/v_{acc}$ is the ratio of slab length subducted per unit time versus the length of accommodation space created for it, by means of the vertical sinking away of older slab and the migration v_o of the trench away from the site of older subduction (see Cerpa et al. 2022, eq. 1, for exact definition). K>1 indicates "traffic jam conditions", where plate convergence is too rapid to be accommodated undeformed, so that slab is forced to thicken (probably by folding). The average value observed for present-day trenches is K~2.5 (Cerpa et al. 2022), with the associated slab types highlighted by grey shaded panels D, F, H. $v_o < 0$ (trench advance, panels B & C) is practically not observed.

Figure 5. Paleo-trenches in absolute (mantle) coordinates, as predicted by the observed slab geometries of Figure 3 if the slabs sank vertically. Slab-to-trench transcriptions are drawn in depth increments of 100 km, using the same depth-to-colour mapping as Figure 3. Tracks of paleo-trench (or arc) locations are shown as thick lines if inferred to be produced by westward subduction, and thin lines if produced by eastward subduction or subduction of ambiguous polarity (mostly Farallon). For laterally extended slabs (FS, FN, CR, presumably produced as in figs 4F/H), the arc lines are shown as dashed when a locus of slab deposition is poorly constrained laterally, for a given depth. The colour bar also shows an indicative mapping of slab depth to time of subduction, using 10 mm/year as a typical, heuristic value for slab sinking rate. The coastlines of NAM reconstructed at times 170 Ma (black), ~80 Ma (green), and present day (grey). Grey polygons indicate slab footprints at 800 km depth (in light grey) and at 1400 km (dark grey). Label SN marks the approximate position of the Sierra Nevada batholith; the arrow denotes possible extents of the Hess-Shatsky Rise conjugate plateau. Arc abbreviations: A = Aleutian, KI = Kula-Izanagi. Purple-grey stars on western NAM mark the previous generation of arcs IMS & NJ, extinct and accreted by 170 Ma.

Figure 6. Tomotectonic constraints on the growth and consumption of ocean basins subducting into the Archipelago from opposite sides. (A) Time frame for 170 Ma (early Archipelago before NAM started moving west) and (B) for 80 Ma (override far advanced, westward subduction almost overridden). Trenches/arcs active at the respective reconstruction times are highlighted with barbs and the colours corresponding to their depths, and are plotted on the basemap of Figure 4, which shows all arc tracks over time. In (A), the lateral gap between the NAM and its nearest slabs (MEZ, ANG) constrains the extents of a paleo-ocean at 170 Ma (the Mezcalera-Angayucham Ocean), whose westward subduction into MEZ/ANG allows NAM to advance westward. The lateral gap between the reconstructed Farallon spreading ridge (isochrons preserved on today's Pacific plate) and its nearest slabs (CR, CR2) constraints the extents of another paleo-ocean, the Farallon Ocean. Orcas Basin is an oceanic microplate inferred to occupy the space between the double-sided, intra-oceanic CR and ANG trenches. (B) By 80 Ma, lateral overlap of NAM with arc tracks indicates accomplished arc collisions and accretions, except in the far

northwest of the ANG arc. Lateral overlap of NAM with the FS slab indicates that the (southern) Farallon trench is flush against the continental margin. The enduring gap between NAM and the CR slab further north indicates that the northern Farallon arc continues to sit offshore (but is in the process of being overridden and converted into a marginal arc, the future Cascades arc).

Figure 7. Arc terranes matched to slabs. Every substantive slab should be associated with a geologically known arc, and every known arc should be associated with a slab. Arc (super-)terranes are shown in their present positions in the Cordillera on the left part of the map. The same arc terranes are schematically reconstructed above their matched slabs and paleo-trenches, in absolute positions relative to the lower mantle. Colour legend gives the interpreted matches of slabs to geologically known arcs. Superterranes, slabs, arcs and trenches are coloured green if associated with Farallon Ocean subduction; orange if associated with Mezcalera Ocean subduction, and red if associated with Angayucham Ocean subduction. The reconstruction time for the arcs and slab walls corresponds to ~170 Ma (before Archipelago override began), except in the case of the SW-ward migrating southern Farallon (Sierra Nevada Batholith) arc, which is shown in several time snapshots migrating across the area occupied by its associated FS slab. North America is reconstructed at 170 Ma, 140 Ma and 0 Ma. Intermontane Superterrane (IMS) and its continental prolongation, the Native Jurassic arc (NJ) are coloured purple; by 170 Ma, their arc activity had ceased and IMS is shown docked against NAM. The interpreted suture of MEZ arcs (Insular & Guerrero Superterranes INS, orange) against IMS/NJ terranes, is represented by a dozen of collapsed oceanic basins coloured cyan and numbered/labeled in the legend.

Abbreviations: Guerrero-Insular arc terranes include WR (Wrangellia), AX (Alexander), PE (Peninsular), GU (Guerrero), WF (Western Jurassic, Western Hayfork, Foothills, and related terranes), SA (Santa Ana). Terranes are associated with Farallon subduction include CG—Chugach; FR—Franciscan; PR—Pacific Rim; SC—Siletz-Crescent; VC—Vizcaino.
IMS Superterrane (purple) includes terranes BM (Blue Mountains, CC (Cache Creek), QN (Quesnel), ST (Stikine) and YTT (Yukon Tanana). NJ (Native Jurassic arc) is the onshore continuation of IMS arcs, as is presumably its along-strike continuation of extensional magmatism in Mexico ("Nazas arc"), shown by purple asterisks.

Figure 8. Collisional deformation since ~155 Ma, when NAM first rode into the intra-oceanic MEZ arc, and welded it onto the continent's westward-subducting margin. **(A)** Progression of deformation in three time slices before, during and after suturing. **At 160 Ma**, arc magmatism above the westward-subducting Mezcalera Ocean, at the leading edge of North America (NAM), adds crust to the Insular Superterrane (INS) arc and lithosphere to the MEZ slab wall. Circa 155 Ma, the last of Mezcalera lithosphere is consumed between NAM and easternmost INS: NAM collides with INS microcontinent, resulting in the Nevadan orogeny **At 140 Ma,** deformation at the California margin and upward truncation of the slab wall. As NAM is still being pulled westward (by intact trench segments in and out of the figure plane), subduction polarity at the collided segment is forced to flip. **At 100 Ma,** subduction has flipped, to eastward beneath the margin. Its slab, deposited by subduction of the Southern Farallon plate), creates an east-dipping blanket (100 Ma panel) as the trench is forced westward in front of advancing NAM. This subduction is building new, margin-hugging arcs that overprint the NAM-INS suture (including the Sierra Nevada batholith). Both north and south of the initial collision site, NAM continues to collide with microcontinental INS, resulting in widening Sevier deformation (Columbian orogeny in Canada).
(B) Generalized cross-section through a continent-beneath-arc suture, such as between NAM and INS. This spatial zoom into the green box in the 140-Ma panel of A is based on a stylized cross section through central Taiwan, a moden example of continent-arc collision with subsequent subduction flip (after Beyssac et al., 2007; section oriented normal to the suture). Both the Taiwan and the INS-NAM

sutures show widespread distribution of units containing old detrital zircons, tectonically exhumed forearc (tectonically removed), and high grade, rapidly exhumed metamorphic rocks immediately inboard of the suture. Kmg is Cretaceous orthogneiss (Chipan gneiss) that has cooled through 240 °C in the past million years (Beyssac et al., 2007).

Figure 9. Margin-parallel terrane translations based principally on paleomagnetic data from Late Cretaceous and Eocene strata. These data constrain the tomotectonic terrane reconstruction model of Clennett et al. (2020), which is modified in the figures. (A) Present-day terrane map shows the current locations of a half-dozen units that are very robustly constrained. The green/blue lines, with nodes every 10 Ma and date labels (in Ma) at key times, represent the spatio-temporal trajectories into the past of these units, back to when they were deposited. A 1000-km scale bar is shown for reference. Trajectories are in absolute coordinates relative to the lower mantle, according to our Clennett et al. 2020 reconstruction. This reconstruction honors the displacement constraints of the most solid paleomag sites, Carmacks & Mount Tatlow/Churn Creek, but Spences Bridge is not honored since it does not fully pass the fold test. The model is based on globally derived apparent polar wander paths (APWP), which reach the same conclusion as for APWP derived solely from North American rock units (Housen, 2021; Tikoff et al., 2022). The *main* BajaBC translations are implemented 70-50 Ma along the yellow line, which runs mainly through Intermontane terranes (and their left-behind correlatives in the Blue Mountains/U.S.). This Baja-BC fault line is necessarily speculative, but it must run inboard of all paleomag sites that show significant offsets (details in section 6.2). The trajectory of the Sierra Nevada, illustrative of a non-translated site on stable NAM, is shown in dark green. Accreted superterrane packages follow the colour scheme of Figure 7; additional pericratonic blocks are colored dark and light purple.

(B) Tomotectonic reconstruction of the assembly of Alaska from Baja-BC and Angayucham terrane translations. This 85-Ma snapshot f the Clennett et al. 2020 model reconstructs the configuration of Baja-BC (comprising at a minimum the terranes west of the yellow line) at the onset of its northward sprint. The locations of the Angayucham (red barbs) and northern Farallon trenches (green solid barbs) are constrained by the ANG and CR slabs, respectively. The terranes of the then-active ANG arc (Koyukuk, future Central Alaska, in red) were welded into the Orcas microplate, but gradually being dislodged and rotated by the obliquely colliding NAM – the "Great Alaskan Terrane Wreck" of Johnston (2001). The northern Farallon arc terranes (Pacific Rim, PR, and others now underplating INS) were also intruded into the Orcas plate and slowly accreted against INS. During its northward sprint, Baja-BC effectively became part of the Orcas plate, separated from NAM by the "Baja-BC fault" (yellow line) or collection of faults.
Baja-BC passes *inboard* of, and unimpeded by, the CR Farallon trench, which still sits offshore. As NAM advances westward, Orcas is squeezed out toward the west or north. It may have subducted into one of two small slabs observed under the grey areas (see text). Due to the small size and mobility of the plate, its disappearance can be rapid, and the Baja-BC and Central Alaskan terranes on it are transported along (the "sprint" phase). As the Orcas seafloor subducts, the northern Farallon trench persists and makes landfall on NAM, becoming the continental Cascades arc by ~50 Ma, which shut off this northwestern passage for shuffling terranes. Baja-BC and Central Alaska collapse against each other and against NAM, completing the assembly of Alaska. The angle between the yellow line (paralleling the NAM margin) and the ANG slab (red line) sets the angle of the Alaskan orocline.

Tomotectonics of Cordilleran North America since Jurassic times: double-sided subduction, archipelago collisions, and Baja-BC translation

Karin Sigloch[1] and Mitchell G. Mihalynuk[2]
[1] Université Côte d'Azur, Observatoire de la Côte d'Azur, CNRS, IRD, Géoazur, 250 rue Albert Einstein, Sophia Antipolis 06560 Valbonne, France
[2] British Columbia Geological Survey, PO Box Stn Prov Govt, Victoria, BC, V8W 9N3, Canada

Abstract

Tomotectonics hindcasts paleo-trenches, through the spatiotemporal superposition of subducted lithosphere (slabs imaged in the earth's mantle) with plate reconstructions (constrained by seafloor isochrons). The two geophysical datasets are linked through the tomotectonic null hypothesis, that oceanic lithosphere sinks vertically down after entering in the mantle. This linkage permits simple and testable predictions about the location and lifespan of volcanic arcs, and specifically, about arc-continent collisions, switches in subduction polarity, and switches from consuming to transform plate boundaries. Tomotectonics uses land geological observations for validation. We explain the tomotectonic method, with a conceptual separation of its (geophysical) hypothesis-generating stage from its (geological) hypothesis-testing stage.

We generate a full suite of tomotectonic inferences for the North American Cordillera from the slab assemblage now occupying the mantle to depths of 1800-2000 km. We reason why this assemblage originated as a completely intra-oceanic archipelago, at a time of worldwide tectonic reorganization around 200-170 Ma, when the Atlantic began to spread, and the Pacific plate was born. The Archipelago was bounded by two sets of trenches that pulled in seafloor from the east/northeast and from the southwest. While on the archipelago's western boundary, intra-oceanic Farallon arcs consumed purely oceanic plate, the eastern boundary arcs pulled in ocean lithosphere that was attached to western North America, until totally consumed. The resulting collision between the continental margin and the eastern bounding arc (which was built on Insular Superterrane) was diachronous, commencing ~155 Ma (Nevadan orogeny), and continuing through the Sevier orogeny times. Upon collision, subduction polarity was forced to flip at the affected latitudes, so the pre-existing Farallon trench grew southward to accommodate the new kinematic requirement for eastward subduction. The new southern Farallon subduction produced arcs on the continental-margin, including the Sierra Nevada Batholith ~120-80 Ma.

Slab-free areas hindcast that this Andean-type margin at U.S. latitudes did not persist beyond ~80 Ma, and that it must have been followed by a dextral transform regime, i.e., by boundary conditions conducive to large-scale terrane translations. This transform regime ended when the northern Farallon arc, still sitting offshore until ~75-50 Ma gradually collided with the margin to become the continental Cascades arc. In the northeastern boundary arcs of future Central Alaska collided with the continental margin 90-50 Ma, and then gradually collided with the northern Farallon arc. Oblique override of these two oceanic arcs produced a range of collision styles, including the Baja-BC northward sprint and the assembling of Alaska. From its combined accounting of arc override events over the past 170 Ma, tomotectonics indicates large-scale northward displacement of Insular Superterrane since its accretion, in direct and independent support for the "Baja-BC" hypothesis of paleomagnetism.

1. Introduction

The term "tomotectonics" refers to a set of quantitative reasoning tools for reconstructing the paleo-geographies of regions shaped by subduction. Tomotectonics aims to account for all observations that record the processes of (paleo-)subduction, above and below the surface, and to reconcile them in a hypothesis-driven framework. Two types of observations play a fundamental role in that they generate the predictions of the tomotectonic method, and they feature in its name: "tomo" (for seismic tomography of subducted lithosphere in the mantle) and "tectonic" (for plate tectonics). These are largely geophysical observations, which are linked by a null hypothesis about vertical slab sinking that generates a shared, absolute spatial reference frame for slabs and plate motions.

Geological field observations play a different role: to test the tomotectonic predictions, and thus to reject or support the hypothesis. Pertinent geological observations are made in accretionary orogens, which are the surface products of the long-lived subduction processes recorded by the slabs. They contain the volcanic arc terranes that are directly and causally tied to the lithosphere that subducted. This paper applies the tomotectonic method to the North American Cordillera, inferring and evaluating its paleo-geographies since Jurassic times, which is the natural limit of scope in terms of confident geophysical observations, both for the mantle beneath North America and for the Farallon plate record surviving at the surface, on the Pacific plate.

The strength of the tomotectonic approach is its particularly simple, strong working hypothesis, which describes the behavior of subducted oceanic plates once they have entered the mantle. With very few degrees of freedom, the vertical sinking hypothesis is highly predictive – and realistically falsifiable, the hallmark of a useful hypothesis. It does not follow that its falsification is easy in practice because the observational database of land geology is so complicated and incomplete. The essence of subduction is to remove its own traces from the surface into the subsurface. By contrast, the inventory of paleo-seafloor deposited in the mantle should be complete. That leaves the practical challenge of imaging it completely with seismic tomography, a domain where major progress has occurred over the past ~20 years (Earth Model Collaboration 2024, Hosseini et al. 2018, Pavlis et al. 2012).

Part 1 of this study, the prediction-generating part, consists of Sections 2-4 (figures 1-6). Section 2 presents the relevant observations from mantle tomography and quantitative, global-scale plate reconstructions. Section 3 explains the tomotectonic working hypothesis of vertical slab sinking, which links the two data sets and renders them predictive. Section 4 carries out this predictive program by hindcasting paleo-trenches and their override sequences for North America.

Part 2 consists of Sections 5 and 6, which examine the predicted arc-building and accretion events in light of geological observations. Section 5 presents the validation principle: that every slab in the mantle predicts a (paleo-)arc at the surface, which should correspond with a geologically observed arc of suitable age, spatial extent and composition (e.g., continental versus oceanic). Equally important, every geologically known arc should be paired with a plausible slab in terms of location and depth. Section 5.3 re-runs the tomotectonic override sequence of Section 4.4 in order to spell out its predictions for the paired, real-world arc terranes.

We have been able to identify only one set of slab/arc matches that leaves no orphaned arcs or slabs, and invokes no more complicated behavior than admitted by the tomotectonic null hypothesis (Sigloch & Mihalynuk 2013, 2017). It has generated significant debate because it predicts more intra-oceanic subduction and later accretion events (Late Jurassic to Cenozoic) for Cordilleran superterranes than more established interpretations (Monger & Gibson, 2019). On the other hand, the established interpretations have all been challenged from within geology as well (Moores 1970, Moores 1998, Johnston 2008, Hildebrand 2009, Schweickert 2015, Tikoff et al. 2023). Here we focus more on inferring large-scale transform motions from major structural breaks in the younger slab assemblage, and non-deposition – pertinent to "Baja-BC" displacements mostly between 80-50 Ma (Irving 1985, Enkin 2006, Kent & Irving 2010, and extending to 100 Ma according to Tikoff et al. 2023). Such displacements obscure preceding terrane accretions and are seemingly at odds with concurrent continental arc construction (Cowan et al., 1997). However, the mantle is very informative and provides a geometric solution to the Baja-BC conundrum.

The reasoning of Section 5 provides the skeptical reader with a template for proposing and evaluating alternative sets of slabs-arc pairings that satisfy the same observations and simple null hypothesis. Alternatively, the reader could envisage the level of mantle convection complexity required to link slabs to surface geology, and whether such complexity yields a predictive working hypothesis.

Section 6 discusses how all collision types in the Cordillera were shaped by double-sided subduction in one form or another: from the early head-on collision in the U.S./Sierra Nevada segment, to oblique collisions during the Sevier orogeny (Columbian orogeny in Canada) and predominantly transform Baja-BC translation.

In this Penrose Volume contribution, we continue to add tomographic tools for deriving past plate kinematics from tomographic images of subducted oceanic lithosphere. We specifically refine techniques for deciphering periods of transcurrent motion from the tomographic slabscape, applying these tools to the BajaBC debate. Section 7 provides a synopsis and considerations for guiding meaningful discussion and work in the future.

2. Observations for a tomotectonic reconstruction of Cordilleran North America

Tomotectonics makes spatial and temporal superpositions of two types of structures that are observable essentially by geophysical means:

1) The 3-D geometries of subducted oceanic lithosphere in the mantle ("slabs"), obtained from seismic tomography.
2) Quantitative reconstructions of plate motions across the earth's surface over time, mainly based on remnant magnetism of extant seafloor.

For North America (NAM) a superposition of slabs and plate motions for the past ~170 million years (Ma) is shown in Figure 1, which serves as a visual roadmap for this study. The translucent patches outline mantle regions (volumes) where subducted seafloor is observed at certain depths between the surface (0 km) and 1800 km. A first-order observation is that slab distribution is uneven, and that large regions of the mantle do not contain slab at any depth. Outlines of the NAM west coast trace the continent's westward drift over the past 170 Ma, as reconstructed by the "Global R" absolute reference frame (Torsvik et al. 2019). If in a thought experiment, a resident of Washington state on the U.S. west coast could be transported 130 million years (m.y.) back in time with the continent, the reconstruction of figure 1 hindcasts that they would end up in a present-day latitude and longitude signaled by the "130 Ma" coastline, an absolute position that is presently occupied by Maine on the U.S. *east* coast.

2.1 Tomographically imaged slabs

Figures 2 and 3 render all slabs (or rather, seismically fast P-wave anomalies) in the teleseismic P-wave tomography model of Sigloch (2011), down to ~1800 km depth in the mantle (where this regional model loses resolution). Mantle imaging under North America made a quantum leap in the wake of the USArray Transportable Array deployment across the (western) U.S., when ~400 broadband seismometers rolled across the contiguous U.S. between 2004-2013 (Meltzer et al. 1999). In more recent tomographies, including global models that image deeper (Hosseini et al. 2018), the resolution under North America remains driven by the USArray data set. Other regional tomographies of North America can be inspected at the portal of (Earth Model Collaboration 2024). The massive slab complexes to be discussed are well delineated in practically all post-USArray tomographies. Imaging differences or uncertainties persist mainly in the shape of less massive, upper-mantle slabs. Examples concern the spatial continuity of recently subducted Cascadia (Farallon) slab (see review of Pavlis et al. 2012), or the vertical delineation of old, stable continental lithosphere against slab in the transition zone below it (both are seismically fast).

Figure 2 renders two 3-D oblique views of the slab complex into which the Farallon (Juan de Fuca) slab subducts today. Slow seismic anomalies, which are proxies mainly for hotter-than-average mantle (e.g., Yellowstone), are not rendered but can be inspected in Sigloch (2011). We prefer these 3D iso-surface renderings to the more commonly seen 2-D depth slices ("red-blue" maps) because vertical continuity of structure is particularly important in tomotectonics. The disadvantage of oblique views is that their 3-D content cannot always be presented satisfactorily on 2-D paper. As a compromise, we show the same 3-D renderings in "map view", with the virtual camera pointing vertically down – as in Figure 3a, or up as in Figure 3b. With color as a proxy for depth, such "3-D map views" convey the vertical connectivity of structures, and easily tie to surface map overlays. The "inside-out" map view of Figure 3b renders the deepest (red) slabs in the foreground, unobscured by the blanket of shallower slabs. The deepest slabs (1100-1800 km, red to yellow levels) are very steep and spatially concentrated in linear belts. We call them "slab walls". By contrast, slabs above 1000 km show more lateral spread and are less clearly structured. To get oriented in the 3-D renderings, the reader may find it useful to match the slabs cartooned in Figure 1 with the 3-D slab observations in Figures 2 and 3. In section 4, we consider these slab geometries in detail, after discussing in section 3 how we propose to interpret their evolution over time and space.

That seismically fast anomalies (below lithospheric depths) represent subducted lithosphere has become a quasi-certainty as imaging resolution has improved over the decades. Lots of lithosphere is expected under North America from its subduction history, and at least recently subducted slab should remain tomographically visible. Indeed, fast anomalies are now unfailingly imaged in the upper mantle below subduction zones (e.g., the purple slab level beneath Cascadia in Fig. 2). These fast anomalies coincide with the band of seismicity produced within the slab in the upper mantle (<700 km depth), which ground-truths the tomographic detection of slab. The imaged anomalies usually continue below the deepest earthquake depths, and this satisfies *a priori* expectations from geologic or plate tectonic records of longer subduction histories (at least 180 m.y. in the case of the northern Farallon slab of Fig. 2). Finally, there is no plausible alternative for what the fast anomalies might represent other than cold, subducted lithosphere.

2.2 Quantitative plate reconstructions

The primary constraints on quantitative plate reconstructions come from paleo-seafloor spreading ridges. Their spreading histories are recorded as isochrons ("stripes") of alternating seafloor magnetization, which in principle permit very detailed and accurate reconstructions of relative plate motion circuits as long as plates can be linked through paleo-spreading ridges. The activity of trenches destroys these records by subducting the magnetized seafloor. Hence isochron-based reconstructions do not reach back beyond 100-200 Ma, but for North American reconstruction, the situation is very favorable. We require mainly the (completely preserved) Atlantic spreading record, which is completely preserved back to Pangean times (>170 Ma, Müller et al. 2008). For eastward subduction, constraints are provided by an exceptionally long (>180 Ma) record of Farallon-Pacific spreading in the Pacific basin (Engebretson et al. 1985), although with the Farallon plate now subducted, we must rely on an assumption of symmetric spreading, which is well supported observationally (Müller et al. 1998).

Seafloor isochrons only permit reconstructing the paleo-plates' motions *relative to each other*. It is crucial to appreciate that the reconstruction of Figure 1 is delivered in *absolute* coordinates relative to the lower mantle. The lower mantle is chosen as reference because it is the most slowly changing among the earth's layers, moving 1-2 orders or magnitude more slowly than tectonics plates, i.e., millimeters per year, versus several centimeters or more. The absolute tie of relative plate circuits to the lower mantle is achieved via intraplate hotspot tracks: the entire lithospheric shell of the earth must be translated relative to the deeper mantle over time, such that in the reconstruction for time T, all seamounts dated to time T in the available hotspot tracks come to overlie the *present-day* positions of their generating hotspot volcano. The mantle plumes presumed to create the volcanic hotspot tracks are expected *a priori* to originate as upwellings from the lowermost mantle. Therefore, the reasoning becomes that hotspot tracks empirically yield the best available proxy for the quasi-stationary lower mantle. Indeed, the set of (Indo-Atlantic) hotspots is observed to have moved only very slowly relative to each other (<10 mm/yr) (Morgan 1983, O'Neill et al. 2005). The simplest explanation is that the hotspots do not move relative to the medium in which they are anchored, i.e., the lowermost mantle. The specification of "Indo-Atlantic" hotspots is important because North American paleo-positioning in Figure 1 is achieved relative to this well-behaved, near-stationary set of hotspots of the Pangean hemisphere. Pacific hotspots, whose stationarity is more questionable (Wessel & Kroenke 2008), are not needed and do not enter any of our reconstruction arguments. Pacific hotspots are not used to infer the sequence of North America drifting and override of the intra-oceanic archipelago that we infer from slab geometries.

3. The tomotectonic null hypothesis of slabs settling vertically

3.1 Predictive power of the vertical sinking hypothesis

Tectonic plates at the surface move horizontally, at typical velocities of centimeters per year relative to the lower mantle (or rather, relative to hotspots, our best proxy of lower-mantle motion). A way of defining vertical slab sinking is that a sliver of tectonic plate loses all of its horizontal motion upon entering its trench, and subsequently moves only vertically down under the pull of gravity (Fig. 4a). An analogue would be a tablecloth draped too far over the edge of a table, and which starts sliding off the table under the pull of gravity. The part of the cloth still covering the table is moving horizontally, but at the table edge (the "trench"), its motion is abruptly converted into almost exclusively vertical motion, until all of the cloth has "subducted" off of the table. For this change of the motion vector to occur, the table cloth needs to be pliable; if instead it was stiff like a sheet of metal, motion vectors for portions above and astride the table would be identical. A defining characteristic of a tectonic plate is that it does behave like a stiff sheet at the surface, in principle not admitting internal deformation. Hence the vertical sinking hypothesis postulates that a plate entering the mantle in a subduction zone loses rigidity and deforms to follow only the pull of gravity, because stress transmission from its still-connected, surficial part has become ineffectual.

We first consider the utility of vertical slab-sinking behavior in paleo-geographic reconstruction that follow from the example of slabs beneath North America in figures 1 & 3. The vertical-sinking hypothesis predicts that every latitude and longitude where slab is observed (at any depth) must once have hosted a paleo-trench and its arc at the surface. The slabs map out their own paleo-trench locations (vertically above them), although we need more information to determine when each trench was actively depositing slab. It is equally straightforward to hindcast the absolute locations where no trench was ever present, namely above the slab-free areas in figs. 1 & 3. No other method of inference provides such straightforward predictions of paleo-trench and -arc geometries. (In this paper, we variably refer to paleo-trenches or paleo-arcs in terms of predictions, sometimes interchangeably. Every subduction zone where plate is consumed must feature both a trench and an arc on the overriding plate – running in parallel, typically spaced by 80-200 km, which is a small distance compared to observational uncertainties in paleo-reconstruction. In the hypothesis-generating, geophysical sections 3 and 4, we typically refer to paleo-trenches being predicted (i.e., plate boundaries), whereas in the hypothesis-testing, geological sections 5 and 6 we refer more to paleo-arcs, as the most survivable and localizable record of the paleo-plate boundary.

The joint consideration of slab geometries with the continent reconstruction of Figure 1 extends the predictions to the type of plate boundary. Recall that the west coast in Figure 1 is reconstructed relative to the lower mantle. Under the vertical-sinking hypothesis, the (lower-mantle) slabs of Figure 1 have not moved laterally since entering their trenches. Hence the slabs and the continent are shown in the same, lower-mantle reference frame, and their absolute coordinates are directly comparable.

Under this hypothesis, the passage of reconstructed North America across the slab-scape in Figure 1 directly translates into a paleo-movie of the continental margin riding into a network of subduction zones. The trenches (slab-filled areas) can only have existed while the continent was not occupying their positions. By the end of the movie (0 Ma), all slabs must have been deposited in their observed positions, vertically below a network of paleo-trenches, the positioning of which must respect plate geometries and other plate tectonic rules. For example, if the orange, northern MEZ slab now located under the U.S. eastern seaboard sank vertically, it could not have been deposited after ~90 Ma because by that time, the continent was overlying all areas occupied by the slab. Hence no trench or arc younger than ~90 Ma can be assigned to those easterly absolute longitudes in a tomotectonic reconstruction. By the same argument, a paleo-trench must have been overlying, or migrating across, the absolute area now occupied by FS slab, and it must have been active before ~70 Ma, because by 70 Ma, the continent was overlying the entire area occupied by FS slab. Between ~170-150 Ma, the west coast traversed a slab-free zone, hence a trench along the west coast is not admissible for those times. For times more recent than ~150 Ma, increasingly large segments of the west coast overlap slab provinces (MEZ, ANG, FS), which means that a trench is required at those times and latitudes along the margin, Andean-style. If FS slab, for example, was laid down after ~130 Ma, then it must have been generated by eastward subduction; the sourcing of slab from west of FS would be inconsistent with NAM occupying this region by ~130 Ma. The vertical slab sinking hypothesis is testable in principle: if somehow, we could be sure that slab FS was deposited more recently than 70 Ma, we would have to conclude that the slab must have sunk significantly non-vertically, translated eastward in the mantle (unless the continental reconstruction was in error, placing NAM too far west).

3.2 The range of slab geometries generated by vertical sinking

There are two conditions for vertical slab sinking: (1) a plate must lose its rigidity upon entering the mantle, and (2) while sinking in the mantle, the slab does not get advected laterally by ambient mantle flow. These conditions may well be met, not perfectly but within the observational uncertainties. A crucial (tomographic) observation in this context is that slabs are much thicker than a single sheet of mature ocean lithosphere (i.e., much thicker than ~100 km) if they are located in or below the mantle transition zone, i.e., below ~400 km depth. Hence the question becomes whether the thickened slabs sink vertically within the observational uncertainties. We can limit the null hypothesis of vertical sinking to thickened slabs, since in tomography models, slabs appear ubiquitously thickened from the mantle transition zone down (figs 2 & 3).

This section considers the first condition of slab softening near the trench, leaving the second question of lateral entrainment to section 3.3. Historically, vertical slab sinking has served as the physically plausible starting position from first principles; deviations from it were considered as and when required by observations. The first-ever cartoon of subduction, published by Harry Hess (1965) and reproduced in Figure 4A, spells out vertical sinking beneath a moving trench. Hess conveys the concept of softening with clarity by envisaging a slab as a chain of viscous droplets, each of which should sink vertically if they are relatively dense and not entrained by pre-existing, lateral motion of the low-viscosity mantle through which they sink. The trench in Figure 4A has moved from points A to B, *relative to the mantle*, and Hess spells out how the ratio between trench velocity and slab sinking rate determines the slab dip angle: "If the overriding continent or island arc moved forward at the same rate that the current [i.e., droplet] descends then a plane dipping at 45° will represent the zone along which the motion is taking place." An unrealistic aspect of Hess' cartoon, published a few years before the plate tectonics breakthrough of his postdoc (Morgan 1968), is that the subducting plate does not actively converge onto the trench (zero motion relative to the mantle). Hence it has no horizontal velocity to lose upon entering the mantle, whereas actual subducting plates are typically observed to move trenchward several times faster than their overriding plates (Forsyth & Uyeda 1975, Cerpa et al. 2022). Figure 4, panels B-I explores the slab geometries predicted to result from vertical sinking as a function of the velocities v_{sub} and v_o of the subducting plate and overriding plates, respectively (keeping the slab sinking rate v_z constant in all scenarios). This regime diagram includes the most frequently observed regimes where v_{sub} is significantly faster than v_o or v_z (panels B, D, F and H).

The geometrically simplest case (Fig. 4E) is vertical sinking under a stationary upper plate and arc (v_o=0), with a relatively slow subducting plate. This results in a vertically dipping slab, which remains undeformed because the rate at which it enters the mantle is fully accommodated by the vertical removal of older slab through sinking: $v_{sub} = v_z$, with v_o=0. By contrast, the mantle entry rate in Figure 4D much exceeds the sinking rate ($v_{sub} = 2.5v_z$, a typical value for present-day subduction zones, Cerpa et al. 2022), and this excess of subducted lithosphere is accommodated by slab thickening ("shortening") – most likely through a folding process, as cartooned (Ribe et al. 2007, Stegman et al. 2010). The result is a thickened slab that dips vertically, since the trench is stationary.

Vertical sinking under migrating trenches ($v_o \neq 0$) results in dipping slabs (Fig. 4B/C, F/G, H/I), the dip angle determined by the ratio between trench motion v_o and sinking rate v_z, as already noted by Hess (1965). Whether or not a dipping slab is thickened again depends on whether the slab entry rate exceeds the rate at which accommodation space is generated in the mantle. Not only slab sinking out of the way (v_z), but also lateral trench migration $v_o \neq 0$ contribute to accommodating the slab in this generalized scenario. The "traffic jam" conditions that result in slab thickening prevail in most present-day subduction zones (Cerpa et al. 2022): plate convergence is typically 50-100 mm/yr, of which only one half to one quarter can be accommodated by vertical slab sinking and lateral trench motion. Thus, thickened slabs are expected *a priori*, and are indeed observed: the slabs contoured in figs. 2 & 3 are several times thicker than a sheet of lithosphere, except immediately below the Cascadia trench (purple in Fig. 2).

We interpret the massive slab walls MEZ, ANG and CR/CR2 in Figure 3B to have formed similar to Figure 4D, and slabs FS and FN to have formed as in Figure 4F. Very rapid convergence in Figure 4H produces a flatly subducting slab, a regime which may apply to part of FS slab (Laramide flat subduction episode). While most slabs are predicted and/or observed to thicken, tomography cannot (yet) resolve their internal structure, e.g., the individual folds. For the slabs' continued sinking behavior, it makes no difference how exactly they thickened, but this likely happens by folding (as cartooned), a process shown to be viable and probable by numerical and physical experiments (e.g., Ribe et al. 2007, Stegman et al. 2010, Cerpa et al. 2022). The physics are those of a viscous thin sheet (lithosphere) encountering a semi-rigid backstop (the lower mantle) – sometimes observed when pouring honey or cake batter.

Slab thickening is a viscous deformation process; at the depth where it is observed the lithosphere has lost its "plateness". For the currently subducting Farallon (FN) plate, thickening is observed ~400 km under the well-illuminated Cascadia trench (Fig. 2, or more clearly in Sigloch et al. 2008, their Fig. 1). While softening at 400 km depth is not the same as immediately after trench entry, the difference is small for paleo-reconstruction (even less when reconstructing arcs, which form above lithosphere that has already subducted 80-200 km). A massive slab wall should consist of many lithospheric folds, and the sheet from the trench down to the slab merely corresponds to the next limb to be laid down on the slab wall (Fig. 4D). The laying down of the limb implies non-vertical motion, on the scale of the lateral width of the slab wall (400-700 km). Hence the width of a slab wall represents a quantification of the deviation from strictly vertical sinking (in the upper mantle), and the resulting spatial fuzziness needs to be evaluated together with other spatial uncertainties concerning, e.g., the hotspot frame, plate reconstruction, or the shape of the continental paleo-margin before it encountered the arc, and changes thereof during collision or extension (quantified by Sigloch & Mihalynuk 2013, Supplementary Information). Reconstructing the paleo-arc centered above the slab wall probably entails 100-200 km of uncertainty (the arc might have been shifted towards the downgoing or the overriding plate). But this uncertainty is small compared to other interpretable geometries of interest, such as slab length along strike, or the slab-free gaps between two slabs. Despite the widened slab geometries, the overall slab-scape in Figure 3 remains highly structured, with individual slabs well separated.

3.3 The vertical sinking hypothesis for thickened slabs

The width of a slab wall signals and quantifies a moderate amount of non-vertical sinking in the uppermost mantle, associated with the thickening/folding process. Once a slab is thickened, it is not expected to undergo much additional lateral displacement during its continued sinking towards the core. The wider a slab (wall), the more massive it is and the more nearly vertically it is expected to sink because gravity, vertically down, is the only primary force driving mantle convection. Lateral mantle flow ("mantle wind") is a secondary effect that translates material between regions of (active) downwelling or upwelling. Even if lateral flows were pronounced, they are not likely to effectively entrain thickened slabs because those are the most massive sinkers in the mantle, and because the ambient mantle is less viscous and will therefore tend to flow around a slab in toroidal motion rather than carrying it along.

Lateral entrainment can be quantified by numerical modelling, although a fully realistic setup – 3-D spherical geometry; self-consistent, spontaneous plate formation and subduction rather than forced plate motions; sufficient rheology contrasts in the upper mantle to produce slab folding – remain beyond today's computational possibilities. Van der Wiel et al. (2024) found 2 mm/year average lateral displacement for 10-15 mm/year vertical sinking in the lower mantle, which translates to 266-400 km of lateral displacement while sinking through the lower mantle. As a caveat, their slabs did not fold nor thicken significantly until the lowermost mantle, biasing upward the lower-mantle value (of 2 mm/year) for lateral displacement. If folding had happened in the upper mantle as observed by tomography (and achieved in a 2-D model by Cerpa et al. 2022, through the implementation of an asthenosphere), then the resulting, more massive slabs would probably have incurred even less lateral motion in the lower mantle. In a physically much more approximate setup, Steinberger et al. 2012 also obtained several hundred kilometers of lateral slab displacement during sinking from surface to core. In summary, models are not fully realistic but point towards several hundred kilometers of lateral slab displacement while sinking through the lower mantle, which may still be an overestimate.

A strong observational indicator for vertical sinking, in both upper and lower mantle, is that the slab walls of Figure 3B have remained so vertical and structurally intact, despite their great "height" of >1000 km in places (MEZ, ANG) and their great age (proportional to the amount of lithosphere they contain). By far the simplest explanation for the formation of these slab walls is vertical sinking beneath a stationary arc-trench system (Fig. 4D). The alternative of non-vertical sinking (plus a non-stationary trench exactly compensating for this non-vertical sinking) seems contrived, especially considering the massive slab volumes that would need to have moved around laterally. To remain vertical into the lower mantle, entrainment into lateral flow could not have been significant without destroying the observed vertical wall geometries of Figure 3A/B.

We conclude that first-order considerations, observations and simulations all point to vertical sinking of slabs through the upper and lower mantle, with lateral deviations not exceeding a few hundred kilometers, a small amount relative to slab dimensions of 10^3-10^4 km. Most non-vertical sinking is probably due to the thickening (folding) process in the upper mantle, with the subsequent descent of thickened slab even more nearly vertical. While remaining a hypothesis, this proposition is likely to accrue more support from simulations and from tomotectonic analyses in other regions. Vertical sinking of lower-mantle slabs makes very strong predictions about paleo-geography at the surface. Even where predictions contradict widely held *interpretations* of Cordilleran geology, they are worth pursuing because the vertical sinking hypothesis is so plausible and because the resulting inferences arising from it are straightforward, detailed and geologically testable.

3.4 Vertical slab sinking not tenable for North America?

We have repeatedly encountered a perception that for the slab assemblage under North America, vertical slab sinking has been rejected conclusively. This would be correct only if framed by the current consensus interpretation of paleo-geography: "Vertical slab sinking beneath *an always margin-hugging Farallon trench* is untenable" – whereas for intra-oceanic subduction of the early Farallon and other plates, the question had not been asked. Tomographic interpretations that guided geodynamic models prior to Sigloch & Mihalynuk (2013) had not considered anything but margin-hugging Farallon subduction, and have indeed shown that vertical sinking under a margin-hugging, migrating trench would have generated slab assemblages significantly different from the observed (Lithgow-Bertelloni & Richards 1998) – more evenly spread beneath the continent, rather than concentrated in slab walls with strikes not resembling the contour of the ancestral western continental margin. Bunge & Grand (1997) attributed this mismatch to one specific episode of non-vertical sinking, namely flat subduction during Laramide times (they used ~70-40 Ma), although their numerical forward modelling did not actually produce the postulated, non-vertical sinking. Liu et al. (2008) did achieve highly non-vertical sinking for the same Laramide scenario, but only by replacing forward modelling of Farallon subduction with adjoint (inverse) modelling, and by additionally adopting an unusual mantle rheology *a priori*. Whereas forward modelling predicts present-day slab geometries by numerically subducting plates over a past time period, adjoint modelling solves for paleo-mantle structure at the simulation's starting time (tens of m.y. ago), by minimizing the misfit between observed and simulated mantle structure at present day. Specifically, Liu et al. (2008) investigated whether a paleo-mantle state could be found that was capable of driving sufficiently effective lateral flow to translate the Laramide Farallon slab eastward in the upper mantle (into the MEZ slab), given that the (margin-hugging) trench was too westerly to deposit MEZ slabs in forward models (Bunge & Grand 1997). Hence the adjoint model was basically asking for lateral slab displacement. It could in principle conclude that non-vertical sinking was physically possible *if all input boundary conditions (including paleo-trench locations) were correct*. It could not diagnose *whether* the simulated paleo-trench locations were correct, even less whether non-vertical sinking was actually required. For the same reasons, the adjoint modelling recently deployed by Fuston (2022) cannot diagnose that non-vertical sinking is required in the real mantle – unless it was certain that their *a priori* placement of paleo-trenches (for explaining Insular superterrane evolution) was correct. Note that "flat slab" subduction, which we consider very likely for Laramide times (in agreement with Liu et al. 2008, Humphreys, 2009; Humphreys et al., 2024) can alternatively be produced by *vertical* sinking combined with very rapid lateral trench motion, Figure 4H/I.

Bunge & Grand (1997) or Liu et al. (2008) could not have envisaged anything but a margin-hugging Farallon trench, which justified their escalation from forward to adjoint modelling in order to obtain sufficiently non-vertical sinking. The Cascadia slab of Figure 2 had not yet been imaged, and thus the slab walls under the U.S. eastern seaboard and across Canada ("MEZ" and "ANG") appeared to be the only possible resting places for 180 m.y. of demonstrated Farallon subduction. For lack of additional slabs, MEZ-ANG slabs needed to be matched with the Farallon plate, and the trench must have been margin-hugging from plate kinematics. This situation fundamentally changed with the imaging of the Cascadia (FN/CR) slab into the lower mantle (Sigloch et al. 2008) – a slab that currently receives Farallon lithosphere and arguably always has (c.f. section 4). This discovery made it possible and necessary to question the margin-hugging nature of the (northern) Farallon trench, and to envisage additional intra-oceanic trenches (Sigloch & Mihalynuk, 2013). Hence it is natural to revisit the physically appealing and predictive hypothesis of vertical slab sinking under North America.

3.5 Uniformity of slab sinking

There is no need to hypothesize further specifics about slab sinking, and in particular, no stipulation of any sinking rates *a priori*. If deeper slabs are found spatially adjacent to shallower slabs, there is an intuitive expectation that the deeper slabs subducted earlier, because all slabs sank through essentially the same medium. We will occasionally use this expectation to arbitrate between two explanatory alternatives (e.g., for slab W), but there is no need to elevate this expectation to a part of the hypothesis. The slabs will turn out to embody this principle automatically, e.g., deeper slabs where trenches are known to have been in the deeper past.

There are many opportunities to *estimate* sinking rate from the slab geometries –we present some, and proper quantifications can be found in Sigloch & Mihalynuk (2013) and Mohammadzaheri et al. (2021). These estimates indicate that the slabs sank at ~10 mm/yr (±2 mm/yr), more or less everywhere across the Americas, which is a remarkably uniform result. It has led to misconceptions that tomotectonics *assumes* or imposes a sinking rate arbitrarily. To counter this impression, the present study limits mention of sinking rate, leaving it largely implicit in the tomotectonic observables. An explicit sinking rate is only needed when making an actual tomotectonic movie, where slabs grow at a rate commensurate with plate advances (e.g., Sigloch & Mihalynuk 2017) – in which case ~10 mm/year is the only value that "works" with vertical sinking.

We finish with a single striking observation that suggests a basically uniform sinking rate: the deep ends of the slab walls of figure 3b all reach to 1800-2000 km depth, across the entire study domain. (The regional tomography of figs. 2 & 3 loses resolution around these depths, but global-scale tomographies confirm 1800-2000 km as the deep ends of these slab walls (Hosseini et al, 2018). Below 1800-2000 km, copious volumes of slab are present into the lowermost mantle, but in geometrically different arrangements. This suggests a comprehensive and relatively sudden reconfiguration of paleo-trenches across the area, *plus a constant sinking rate across the domain*, otherwise the slabs that were deposited after the reconfiguration event (and which are the subject of our study) would not all have reached the same depth of ~1800-2000 km. What was this event? Section 4 will yield the answer without reference to a sinking rate, but at 10 mm/year, a slab depth of 1800 km translates to a mantle entry time of 180 Ma. This is the time when Central Atlantic opening started appreciably, setting North America on its westward drift, and also when the Pacific plate (and possibly the Farallon plate) were born – indeed a major reconfiguration that may have fundamentally reset paleo-Pacific subduction zones. These observations are all mutually consistent – supporting uniform slab sinking, as well as clear correspondences between deep mantle structure and known, major surface events. The slab breaks at 1800-2000 km depth thus provide a natural limit for the scope for our reconstruction. An older archipelago, below ~2000 km, is not as sharply resolved by tomography, and the uncertainties on absolute paleo-positioning at the surface (in absence of hotspot tracks) become unworkable beyond Jurassic times.

4. Tomotectonic reconstruction of North America

4.1 A western and an eastern slab complex under North America

We are ready to execute the predictive stage of tomotectonics. One by-product is Figure 5, which makes paleo-trench predictions by "transcribing" the slab-scape of Figure 3 using the tomotectonic null hypothesis. The tomography model is sliced into horizontal maps in depth increments of 100 km. At each depth, a paleo-trench line is drawn above every slab present, and colored according to the depth-to-color scheme of Figure 3. For slab walls, it is easy to draw the inferred trench lines (centered inside the narrow slab). For the almost vertical slabs, the lines change little with depth, resulting in tightly clustered lines in Figure 5. For dipping slabs, the transcription is subject to larger uncertainties, and paleo-coastlines or interpolations may also be used, as will be explained.

The assemblage of slabs under North America clearly separates into two groups (Figs. 1 and 3): a Western Slab Group comprising slabs CR, W and FN; and an Eastern Slab Group, comprising slabs MEZ, ANG, and FS. Slabs within each group are spatially connected and separated from the other group by slab-free mantle.

Figures 1 and 3a show a small overlap between the two slab groups (easternmost CR and westernmost FS), but only laterally, not in depth. This does not violate the vertical sinking hypothesis: the area hosted two different trenches, at different times. The older trench deposited the deeper CR, and the more recent trench deposited FS. The deepest slabs in both groups are slab walls (MEZ, ANG, deep CR), and they all reach to the same depth of 1800-2000 km (magenta color level in Fig. 3b).

4.2 Tomotectonic reconstruction of the Western Slab Group (northern Farallon slabs)

The three slabs of the Western Group (FN, CR, and W) are jointly rendered in Figure 2. The view angle of Figure 2a emphasizes spatial continuity, making clear that the three slabs form a single system that slopes down to the east. By contrast, the view angle of Figure 2b highlights intra-slab breaks and structural divisions. Slab W is seen to be a separate fragment in Figure 2b, but clearly in a spatial correspondence with CR in Figure 2a. The subdivision of the main slab into FN and CR in Figure 1 may seem arbitrary from Figure 3a (FN is the upper-mantle part, corresponding to the purple, light and dark blue levels), but Figure 3b shows that this upper-mantle slab is almost "floating" freely, due to gaps towards the slab components surrounding it.

For visual clarity, Figure 2 masks out certain slab parts by comparison with Figure 3, which renders *all* seismically fast structure (below 400 km depth). Figure 2 omits the deep slab fragment CR2, west of today's west coast. It also masks out an upper-mantle slab that strikes east-west under southern Saskatchewan, Alberta and B.C. (dark blue in Fig. 3a), and which does not participate in the sloping continuity of the Western Group but rather seems to rest on top of it. (We later return to this slab as the speculated Orcas slab.)

4.2.1 FN slab – northern Farallon slab in the upper mantle, margin-hugging trench

"FN" stands for Farallon North. Near the trench, the slab must represent Farallon lithosphere because the Farallon (Juan de Fuca) plate is subducting into it today. Below the present-day coastline of the Pacific Northwest in Figures 2 and 3, shallow slab is imaged beneath the active Farallon (Juan de Fuca) subduction, but neither north nor south of it. This provides a first reassurance that the tomography "works": a slab is imaged below a confirmed (present-day) subduction zone, no slab is imaged below adjacent non-subduction zones.

For depositing the upper-mantle slab FN to the east of the trench, a margin-hugging trench is the only plausible scenario i.e., a continuation of the present-day situation into the past. The continental margin gradually traversed FN slab over the past ~70 m.y. (Fig. 1), and FN slab shallows to the west (Fig. 2a). Westward shallowing is consistent with deposition of FN under a westward migrating (marginal) trench, so that easterly FN is deeper because it had more time to sink, as in fig 4F.

Magnetic isochrons on the Pacific plate trace the growth of the (northern) Farallon plate from ~180 Ma to 0 Ma (Atwater, 1989; Engebretson et al., 1985), spreading towards the Western Slab Group. Since these slabs represent the paleo-trenches closest to the reconstructed Pacific-Farallon spreading ridge over time (e.g., Engebretson et al., 1985, Seton et al., 2012), and since Farallon plate is still subducting into this slab today, the Farallon plate must have subducted into FN in the past as well.

In summary, FN holds Farallon lithosphere, and today's Farallon trench is built on the continental margin. The margin's eastward progression back into the past in Figure 1 matches the FN slab's eastward down dip: everything points to a margin-hugging trench in the past as well.

4.2.2 CR slab – northern Farallon slab in the lower mantle, intra-oceanic subduction

At first glance, lower-mantle CR slab (turquoise levels and below in Figures 2 and 3) seems to smoothly continue the downward dip of FN slab (with a margin-hugging Farallon trench as the explanation), but there are serious problems with this proposal. With increasing depth, CR slab appears increasingly spread out laterally in Figure 2a because at those depths CR is no longer dipping east. Rather it has steepened into a slab wall and rotated counterclockwise relative to FN and the coastline, with its long axis striking NW-SE (especially clear in Fig. 3b). If the deep CR dips at all, it is to the west, in the "wrong" direction for subduction beneath a west-migrating continental margin. Deposition of the voluminous slab wall portion of the CR required a stationary trench striking highly oblique to the coastline (Fig. 1). At yellow/green depth levels in Figures 2 and 3, the CR slab looks segmented and complex, including the detached fragment W – again, not a good match to the paleo-coastline.

CR is much more voluminous than FN, requiring a trench that dwelled in the area, but the coastline did not dwell: by >80 Ma, it shows no overlap with CR slab in Figure 1. The northern Farallon plate was spreading since >180 Ma, meaningthe continental margin outlined in Figure 1 leaves the CR slab 100 m.y. too early to be consistent with the widely held idea of (northern) Farallon plate subducting since its inception (~180 Ma) under North America. Prior to 80 Ma, the NAM margin in Figure 1 traverses the slab-free zone to the northeast of CR, which for tomotectonics implies no trench along the margin. Finally, CR2, an isolated slab as deep as CR, is present just offshore the present-day west coast in Figures 3a and b – further west than the margin ever was – so that CR2 cannot be due to vertical sinking under a margin-hugging trench.

The inevitable conclusion is that CR and CR2 cannot have been deposited into a margin-hugging trench by vertical sinking, unlike FN. Therefore, prior to about 80 Ma, the northern Farallon trench must have sat *offshore* the NAM west coast, or in absolute coordinates, NAM sat well east of the stationary Farallon (CR) trench. Jointly, FN and CR are voluminous enough to account for the observed 180 m.y. of northern Farallon spreading and subduction.

Hence, by coincidence, FN is not only the upper-mantle part of the northern Farallon slab, but also the part that was deposited by an Andean-style (Cascades) trench. CR, the lower-mantle Farallon slab, was deposited by an intra-oceanic trench. The geometric complexities at intermediate depths of CR presumably reflect the prolonged, oblique override of by NAM <80 Ma that gradually "accreted" the CR Farallon trench. This tomotectonic prediction of an offshore Farallon trench in the Pacific Northwest >80 Ma has many implications, including that Baja-BC terranes could have shuffled northward *inboard* of this trench (section 5).

In terms of trench lines for Figure 5, the deep slab wall of CR is easy to transcribe (compare to Fig. 3b). For the dipping FN slab, paleo-coastlines were equated to trench lines since a margin-hugging trench has been inferred. The intermediate-depth (turquoise) trenches above the fragmented, rotating slab were drawn as best guesses/interpolations, and they are almost certainly too simplistic. The strikes of trenches drawn above W are guesswork since the slab lacks a clear strike, and we do not fully understand W's functioning relative to CR. The very deepest (magenta, grey) trench levels of CR are also guesswork – were the two separate slab walls originally connected into one long, E-W striking slab (Sigloch & Mihalynuk 2013)? The strike and shape of the offshore CR fragment is not well imaged. The overall complexity of the Western Group is real and not an imaging shortfall – much of its paleo-geographical meaning remains to be deciphered.

4.3 Tomotectonic reconstruction of the Eastern Slab Group

4.3.1 FS slab – southern Farallon slab in the transition zone and lower mantle

The Eastern Slab Group consists of FS, MEZ and ANG slabs. FS should have subducted more recently than MEZ and ANG, due to its more westerly and shallower position. The paleo-coastline of Figure 1 traverses FS from ~130 Ma (±15 Ma) to ~75 Ma (± 10 Ma?), so deposition must have concluded by the later date. The slab occupies the same depths as lower FN and intermediate CR, for which we have inferred similar dates.

FS slab features a linear, sharp truncation towards its southwest, where the mantle becomes slab free. This truncation (yellow line in Fig. 1, the "Big Break") approximately coincides with the strike of the paleo-coastline at 75 or 80 Ma. The simplest explanation for this coincidence is that the FS trench was built on the margin, and that (vertical) deposition into this marginal trench suddenly stopped at 75-80 Ma. The slab's elongation in WSW-ENE direction, which is the direction of margin advance, likewise suggests that FS was deposited beneath the migrating NAM margin.

In Figure 3b, FS slab tends to deepen toward the east (and the south), albeit irregularly. This also points to deposition below the migrating margin: easterly FS slab regions have had more time to sink. The gentle overall dip of FS suggests that its trench migrated relatively rapidly: FS slab geometry best corresponds to Figure 4H, where the slab flattens in and below the transition zone.

An eastward-subducting, margin-hugging trench during Cretaceous times, just south of the northern Farallon system, must be another Farallon trench. The reason is cartooned in Figure 6. When Farallon-Pacific (FAR-PAC) spreading had just started (time 170 Ma), the associated spreading ridge segment is short (as recorded by Pacific isochrons), so the CR slab is wide enough latitudinally to account for the young Farallon plate (fig. 6a). But over Cretaceous times and by 80 Ma (fig. 6b), the FAR-PAC ridge had extended southward (Atwater, 1989; Engebretson et al., 1985), too far to be accounted for by CR slab only – since CR slab visibly did not grow southward. Hence an additional Farallon trench segment must have developed to the south of CR. In fact, FS slab exactly mirrors the lengthening of the Farallon spreading ridge by a commensurate lengthening of the trench: FS starts out very narrow at the 130-Ma coastline but widens southward to underlie much of the U.S. and Mexican paleo-margins before the 80-Ma coastline reaches the Big Break.

In summary, all aspects of FS point to subduction of the southern Farallon plate over the Cretaceous period (roughly 130-75 Ma), beneath the NAM margin. Fig. 6b sums up Farallon subduction shortly before the Big Break: beneath the continental margin of Mexico and California, but still offshore in the Pacific Northwest.

4.3.2 Slab-free window between the present-day margin and FS slab

Next we consider the significance of the slab free area southwest of the Big Break in fig. 1, extending from FS slab to the current margins of southern California and Mexico. South of the northern Farallon/Cascadia trench, a dextral transform plate boundary runs along the *present-day* margin (the San Andreas system). From Pacific isochrons, Atwater (1970) inferred this transform system back to ~30 Ma, to the reconstructed "landfall" of the PAC-FAR spreading ridge on the margin.

Tomotectonics can diagnose the existence of this same transform regime from the absence of slab beneath the present-day margin (indicating that it is not a trench; and a continent-ocean boundary cannot be a spreading ridge either). However, Figure 1 shows that the slab-free window extends eastward from the coast not only to the 30-Ma paleo-coastline, but all the way to the Big Break, which corresponds to the ~75-80 Ma coastline. Hence tomotectonics hindcasts that a transform plate boundary has held sway along the Californian and Mexican margin since ~75 Ma, when the margin-hugging southern Farallon (FS) trench suddenly shut down in the Big Break event.

Slab W (traversed by the coast ~20-50 Ma) might signal a localized, temporary interruption of this transform regime, but it is unlikely. We noted that slab W is deep and blends into the overall geometries of CR, hence it likely represents older subduction. If slab W does not interrupt the subduction-free period after the Big Break, then the current San Andreas regime along the margin is in full spatial and temporal continuity with the transform regime of ~50-80 Ma that was inferred from rock paleomagnetism to have transported the Baja-BC microcontinent northward (Kent & Irving 2010). This is a straightforward consequence of the wide slab-free window, combined with the vertical sinking hypothesis.

4.3.3 MEZ and ANG slab walls

MEZ slab is among the longest and most voluminous slabs in the whole mantle. It is a gigantic slab wall that runs from northeast Canada to Florida under the NAM eastern seaboard, and from there on to Peru (Fig. 1). MEZ wall is >1,000 km "high" under Florida (occupying depth levels ~1800 km to ~800 km in the mantle column, Fig. 3), but only ~300 km "high" under Nova Scotia (occupying ~1800-1500 km depth).

MEZ lies in spatial eastward continuation of the southern Farallon (FS) slab and continues the eastward-deepening trend, although at a dramatically steeper angle than FS. The intuition might thus be that MEZ represents Farallon plate older than FS. Tomotectonics indicates that this cannot be the case.

The deposition of a voluminous, linear slab wall requires a trench that remains stationary above MEZ for a long time (Fig. 4D). By contrast, the paleo-coastline in Figure 1 marches right across MEZ (and ANG) without dwelling on the slab and without showing any correspondence with the slab's shape. In reverse time, NAM leaves behind FS slab by ~130 Ma. By 150 Ma, the margin leaves behind the eastern promontory of MEZ slab wall and traverses only slab-free mantle until 170 Ma – the temporal limit of our study, when the NAM east coast has reunited by with Pangaea and the Central Atlantic closed (see Fig. 6a).

The swift and oblique march of the west coast across MEZ means that a *margin-hugging* Farallon trench could not have deposited the slab wall by vertical sinking. What about a stationary, offshore Farallon trench, as observed in the case of CR? The problem with eastward (Farallon) subduction into MEZ is that it would prevent NAM from moving westward, away from Pangea, between 170 Ma and the moment it reaches MEZ (which is ~150 Ma at the MEZ promontory, and later further south). The slab-free zone between MEZ and NAM at 170 Ma is occupied by seafloor at the paleo-surface, and this seafloor must subduct in order to let NAM move westward (Fig. 6a). The only slab available to subduct into is MEZ, which means *westward* subduction of the seafloor between Pangaea and MEZ, into MEZ trench.

MEZ slab could, therefore, not have hosted an eastward subducting trench at the same time, meaning no Farallon trench, not even an intra-oceanic one. This is the decisive argument against MEZ as a Farallon slab. Westward subduction into MEZ solves other problems: the huge latitudinal extent of MEZ does not match the short isochron segment of the FAR-PAC spreading ridge recorded for Jurassic times (Fig. 6a). The FS slab, narrowing then disappearing to the east, already explains the history of southern Farallon growth.

By contrast, the north-south extent of MEZ is of the correct length and strike to let all of North America break free from Pangaea at once, and to start moving west ~170 Ma. The northern MEZ segment from Nova Scotia to Florida closely matches the Central Mid-Atlantic spreading ridge in length and strike, and from 170 Ma to today. The situation is cartooned in fig. 6a, which highlights (in blue) the seafloor west of NAM that needs to subduct into MEZ (and ANG).ANG slab served the same role as MEZ, enabling NAM to move west. MEZ trench pulled on the NAM margin at U.S. and Mexican latitudes, whereas ANG pulled on the B.C. margin. As required for this functioning, ANG slab wall is the spatial northwestward extension of MEZ, and very similar in character. ANG strikes oblique to the paleo-margin, and it reaches far to the west. This means that the margin took a very long time to override ANG slab – in Figure 6b, its trench is still pulling on the northern margin at 80 Ma, when MEZ has long been overridden.

4.4 Chronological sequence of archipelago override

Pulling all tomotectonic inferences together, we play forward the "movie" of continent-trench collisions, using Figures 1,3, 5 and 6. All trenches start up around the same time (same depth of ~1800-2000 km), while NAM is still with Pangea, i.e., sometime before 170 Ma (Fig. 6a). All trenches are originally intra-oceanic in the proto-Pacific basin west of Pangaea, where they are free to remain stationary and to build the observed slab walls MEZ, ANG and CR.

MEZ and ANG trenches are exerting a westward pull on the NAM plate, whose western plate boundary is not the continental margin but an ocean basin (the "Mezcalera-Angayucham Ocean" in Fig. 6a). From ~200-170 Ma, the Central Atlantic rifts along a line parallel to northern MEZ slab. Central Atlantic rifting transitions to proper spreading ~170 Ma (recorded by Atlantic isochrons, e.g., Seton et al. 2012). The Atlantic opens at the expense of the Mezcalera-Angayucham Ocean, which narrows by westward subduction into MEZ and ANG slabs.

Around 155 Ma, the NAM west coast at U.S. latitudes starts to collide with the northern MEZ trench, under-riding the MEZ arc and deforming the margin (orange barbs in Fig. 1). The collision gradually spreads in latitude as broader swaths of MEZ arc (and later ANG arc) are overridden (Fig. 1, coastlines at 130, 110 Ma). The gradual override of northeastern MEZ slab ~155-110 Ma is recorded by the westward shallowing slab "ramp" it forms in Fig. 3a: under the 150-Ma paleo-coastline, the slab had 150 Ma to sink since the end of subduction, and its upper truncation now lies ~1500 km deep (red level of the 3-D isosurface in Fig. 3a); under the 110 Ma-line, its shallowest part lies 1100 km deep (yellow level) and has been sinking for 110 m.y. (This ramp is among the best opportunities to estimate slab sinking rate, Sigloch and Mihalynuk, 2013). In Figure 5, the slab ramp translates to trench lines on northern MEZ "retreating" westward, from pink to red to yellow levels: no more trench where the Mezcalera Ocean has disappeared.

At conterminous U.S latitudes, subduction cannot cease with the consumption of all Mezcalera Ocean lithosphere because NAM continues to be pulled westward, by still-active trenches of northern ANG and southern MEZ. NAM is pulled into the area presently underlain by eastern FS slab, which forced the ocean lithosphere occupying this absolute position beneath the advancing U.S. west coast, depositing FS slab. Hence subduction polarity flips along the California/Mexico margin: NAM margin turns into the overriding plate (green barbs in Fig. 1), with Farallon plate subducting underneath it. MEZ and ANG trench segments shrink while FS trench grows along the margin. CR trench (northern Farallon) sat in the same stationary, intra-oceanic position the entire time.

At 80 Ma (Fig 6b), these override events have run their course and things are about to change. The southern Farallon (FS) trench on the margin abruptly shuts down ~80-75 Ma and will never be re-established (Big Break of FS slab). A transform system takes over that evolves into the present San Andreas transform (slab-free corridor). The reason for this shutdown of the continental arc is not obvious, perhaps related to the beginning, oblique collision of NAM with northern Farallon (CR) arc. (Or to plateau subduction (Livaccari et al., 1981; Humphreys et al., 2024) which cannot be inferred purely tomotectonically). At the end of a protracted override (fragmentation of upper CR slab), the seafloor that remained between CR trench and NAM in Figure 6b has been squeezed out, and the northern Farallon trench has "accreted" (by ~50 Ma). It continues as the margin-hugging Cascades trench that is still active today (FN slab).

In the far north, ANG arc is under-ridden by NAM very gradually and obliquely into Cenozoic times, always by westward subduction. Once ANG subduction is completed, the northern margin turns into the transform system that continues to the present day.

5. The match between tomotectonic arcs and geologic arcs

So far, we have used only the tomotectonic observables of slab geometries and quantitative plate reconstructions for making the paleogeographic inferences of Section 4; these are linked together by the null hypothesis of slabs sinking in place. Geological observables remain untapped and an independent data set for testing the tomotectonic hypothesis and its predictions.

The principal link for hypothesis testing is the volcanic arc, which is an inevitable surface manifestation of any subduction zone. Tomotectonics hindcasts absolute paleo-arc locations. If the tomotectonic method works properly, every paleo-arc predicted from slab observations should have an actual counterpart in the accretionary orogen. The converse is equally important: every geologically observed arc should be matchable to a suitable "tomotectonic arc", that is, to a slab.

Figure 7 shows the large-scale assemblage of arc terranes since ~170 Ma that need to be explained along the present-day west coast of North America (left part of the map). Figure 7 also schematically reconstructs the paleo-arc terranes above their matched slabs and paleo-trenches. The chosen set of slab/arc matches will arguably yield the "correct" solution, in the sense that the archipelago override sequence hindcast by tomotectonics in Section 4.4 will terminate with the spatial configuration of today's Cordilleran accreted terranes. The slab/arc associations must also satisfy the geologically known timing constraints during the arc accretion sequence. In Figure 7, the current and former instances of arcs are grouped into superterranes and linked by their unchanging colors over time: Farallon arcs and slabs in green, Insular (INS) & Guerrero (GUE) microcontinents in orange; Intermontane (IMS) microcontinent in purple; and Central Alaskan arcs in red. Our slab/arc matches are justified in sections 5.1 and 5.2.

5.1 Northern and southern Farallon arcs (eastward subduction)

Upper-mantle FN slab must be matched with the Cenozoic, still active Cascades arc (du Bray et al, 2014; Tepper and Clark, 2024; though a continuous arc axis is only apparent since ~40 Ma, see Fig. 1 of Glazner, 2022; or ~45 Ma, Humphreys and Grunder, 2022). This match is straightforward in terms of latitudinal extent, timing, polarity, and continental character.

It is less clear which arc terranes to associate with older northern Farallon subduction, i.e., with the voluminous lower-mantle CR slab, schematically drawn as a deep green patch in Figure 7 in its stationary, slab-wall position and strike. Expected to be intra-oceanic in character and accreted inboard of today's Cascades arc, CR arc may well be best preserved in the subsurface beneath Vancouver Island (Clowes et al., 1987) as the downdip extent of the Pacific Rim terrane ("PR" in Fig. 7; Sigloch & Mihalynuk 2013, 2017).

In addition, parts of CR arc may have been entrained and transported north with BajaBC and the successor transform regime that continues to today (e.g., Baranov-Leech River hypothesis of Cowan, 2003; Garver and Davidson, 2015). That such a big and old slab has only fragmentary arc relics illustrates some practical challenges in making slab/arc matches. However, this is equally true for any accounting of pre-Cascades subduction in the Pacific Northwest from geology or plate tectonics alone. FAR-PAC isochrons record Farallon spreading towards the Pacific Northwest since 180 Ma, irrespective of mantle evidence. If the pre-Cascades arc were postulated to have grown on the margin, the problem of the "missing" arc would be aggravated because such an arc should not be displaced as easily as the intra-oceanic CR arc inferred from tomotectonics.

Another straightforward match is the association of FS slab with the arc that built the Sierra Nevada Batholith (SNB, essentially ~120-80 Ma, Paterson and Ducea, 2015). FS slab fits the timing, subduction polarity and continental nature of the SNB arc. Figure 7 shows this arc in translucent lime green, originating at the eastern tip of FS slab, in the inner corner between MEZ and ANG slab walls. The dashed, retreating trench lines schematically represent the subsequent, southwestward migration of this arc with the NAM margin while the FS slab grows below it. Besides the SNB and allied arc segments, FS slab must also be associated with the Cretaceous arc on INS, which lay north of the Sierra Nevada and has since been translated by Baja-BC shuffling (northward by ~1950 km; Enkin, 2006).

For times younger than the SNB arc, no clear arc axis is observed in the southern U.S. sector, which is consistent with the slab-free region southwest of FS slab. Post-SNB volcanism and magmatism in the region are spatially diffuse instead of linearly aligned, not of typical arc chemistry (see Glazner, 2022).

For completeness, the Pacific plate subducts northward beneath southern Alaska today. This subduction zone has been building the upper-mantle Aleutians slab (Gorbatov, et al., 2000; van der Meer et al., 2018), associated with the Aleutians arc since at least 46 Ma (Jicha and Kay, 2018). This obvious match is mentioned here because Baja-BC shuffling events transported southern Alaska terranes (Insular Superterrane) to its present resting place by ~50 Ma (e.g., Kent and Irving, 2010), just before Aleutians subduction initiated and the Aleutian arc started to grow on and outboard of those newly arrived terranes (northward translation of outermost INS is still happening due to coupling across the active dextral transform margin). Earlier Kula subduction events in that region (presumably matched with KI slab in figs. 5 and 3, (Sigloch & Mihalynuk 2017) do not directly pertain to the present study.

5.2 Arcs associated with Mezcalera/Angayucham westward subduction

Section 5.1 has matched all eastward (Farallon) arcs inferred by tomotectonics with actually observed geological arcs. The tomotectonically inferred arcs (i.e., slabs) remaining to be matched are MEZ and ANG. Conversely, five geological arc systems of Cretaceous and Jurassic age remain to be matched to slabs (Fig. 7), from north to south: the Cretaceous arcs of Central Alaska (Koyukuk); the arcs on the Insular Superterrane (INS: Wrangellia, Alexander and Peninsular terranes); arcs on the Intermontane Superterrane (IMS: Stikine and Quesnel); the Native Triassic-Jurassic arc in the southwestern U.S.; and the Cretaceous arc on the Guerrero Superterrane in Mexico.

At times preceding the main SNB flare-up 125-85 Ma (Paterson and Ducea, 2015), arc volcanism was built on Insular Superterrane (INS) (205-165 Ma, younging eastward; Canil and Morris, 2024). According to paleomagnetic evidence (Kent & Irving 2010), INS lay at latitudes of the southern U.S. and northern Mexico when its Jurassic arc was active, but now occupies an outboard position along the margins of B.C. and southern Alaska – hence the name "Baja-BC" (Irving, 1985) for the margin-parallel shuffling that achieved the displacement between 90 and 50 Ma.

Construction of the "Native Triassic-Jurassic arc" (256 Ma (latest Permian) to 175 Ma) on the cratonic margin of the southwestern U.S. was followed (~170 Ma) by a period of transpression and formation of Middle Jurassic ophiolites (Saleeby and Dunne, 2015). Most workers refer to the Jurassic magmatic rocks as parts of an extensional continental arc (Tosdal and Wooden, 2015; Saleeby and Dunne, 2015; Busby and Centeno-García, 2022), that transitions southward to the opening Gulf of Mexico. What proportion of these arc-type volcanic and plutonic rocks (which typically display extensive interaction with the Proterozoic crust) are true arc versus decompression melts related to extension, is an open question. Zircon geochemistry shows elevated Th/U ratios of Sierra-Nevada-derived Jurassic detrital zircons of southeast California (180-160 Ma, Barth et al., 2013) are atypical of arc zircons from both older, Triassic, and younger, Cretaceous, Sierra Nevadan magmatic rocks, and may be from asthenospheric sources (Tosdal and Wooden, 2015).

Intermontane Superterrane (IMS) in British Columbia, located inboard of INS, hosted another long chain of Triassic-Jurassic arcs (Stikine & Quesnel) that went extinct and were accreted by ~174 Ma (Mihalynuk et al., 2004). Before accretion, IMS presumably formed the offshore, northwestward extension of the Native arc in western USA, judging by their geographic and geological relationship (e.g. Mihalynuk and Diakow, 2020) and their almost simultaneous demise or change to extensional regime between ~170 and ~180 Ma (Barth et al., 2013; Tosdal and Wooden, 2015, see above).

The slab wall of northern MEZ lies in spatial and temporal continuity with FS slab, which was built ~130-80 Ma (fig. 1). Hence the Native arc would be too ancient for a match to MEZ slab, and as a margin-hugging arc it must necessarily have been eastward-subducting, whereas MEZ slab accommodated westward subduction (section 4.3, 4.4). IMS arcs cannot be directly paired with MEZ for the same timing reasons: they do not reach to as young as130 Ma.

The geologic arc to associate with MEZ slab can therefore only be the Jura-Cretaceous arc on INS. This is plausible because INS is not part of stable North America but rather an accreted microcontinent. Hence westward subduction beneath INS is possible *a priori*, but paleo-seafloor east of INS would need to be demonstrated, as a match for the tomotectonically inferred Mezcalera Ocean.

Towards the east, INS is indeed separated from IMS by a belt of "collapsed basins" of oceanic character. Sigloch & Mihalynuk (2013, 2017) made detailed geological arguments why these collapsed basins are suitable to represent the suture of the tomotectonically inferred Mezcalera-Angayucham Ocean (light blue in fig. 7). A dozen collapsed basins are shown on their present-day positions (also light blue in fig. 7), and named in the legend. They have the correct ages (sufficiently young from detrital zircon dating), spatial extent (spanning the length of the NAM margin) and character (mantle slivers outcropping in half of the basins) in order to represent the suture of the Mezcalera-Angayucham Ocean that closed west of MEZ slab by westward subduction.

MEZ slab wall runs south to Mexican latitudes. There are suitable geological matches in the Cretaceous arc on Guerrero Superterrane, a southern correlate of INS Superterrane (fig. 7). The collapsed basin representing the Mezcalera ocean (and its suture) to the west of Guerrero is the Arperos basin, adopting an interpretation of Tardy et al. (1992) and Dickinson and Lawton (2001). An additional Mexican arc, the Early Cretaceous Alisitos arc that preceded Farallon subduction (accreted outboard of Guerrero arc) is considered out of spatial scope but is matched to slab by Clennett et al. (2020).

The Cretaceous arcs of Central Alaska are a straightforward match with ANG slab wall. Figure 1 shows how NAM underrode ANG slab very slowly over Cretaceous times and into the Cenozoic – a prolonged, oblique collision that would have slowly plucked the originally linear, >3,000 km long arc off its slab and crumpled its slivers into the tightly folded oroclines seen in figure 7 (in red). The northerly latitude of ANG slab ensures that Central Alaska accretes north of all Farallon and MEZ arcs, as observed. This huge slab provides a satisfying placement for Central Alaskan terranes that have been difficult to place or to relate to more southerly events in reconstructions based purely on geology (e.g. Patton and Box, 1989) or purely on plate reconstructions (e.g., Seton et al. 2012).

With this, all arcs back to ~170 Ma are matched to slabs, and all slabs in figure 1 are matched to arcs. The two oldest candidate arcs, Native arc and IMS (Stikine, Quesnel), remain unmatched to slab. This is unsurprising in light of our tomotectonic inference that the Archipelago to 1800 km depth records events since Pangaean breakup and Atlantic spreading. The ~170 Ma extinction of a long, linear chain of Native/Intermontane arcs, and its sudden replacement by the even more vast MEZ and ANG arcs, must be a consequence of hemispheric reconfiguration of the time. Sigloch & Mihalynuk (2017, 2020) speculatively matched slab below the Atlantic to the Native/IMS arc, albeit not directly below the 170-Ma position of NAM in fig. 1. The uncertainties of absolute paleo-positioning multiply into Jurassic times, with neither surviving seafloor nor hotspot tracks available, and lingering questions about True Polar Wander (Fu & Kent, 2018).

5.3 Archipelago override sequence replayed with arc terranes

We replay the archipelago override sequence of Section 4.4 with the matched geologic arc terranes. The most relevant figures are figures 7, 6 and 5. Events are narrated with an emphasis on slab pull as the driving force. This is justified by the observation that 90% of present-day plate motions can be explained by trench configurations: plates mainly seem to move because they are pulled perpendicularly into subduction zones where dense slab is sinking into the mantle (Forsyth & Uyeda, 1975).

In the proto-Pacific basin, a vast grouping of intra-oceanic arcs starts up relatively simultaneously between 205-180 Ma. This new Archipelago sits >1,000 km west of NAM and consists of arcs that built the Insular-Guerrero Superterrane, a Mesozoic-Paleozoic microcontinent; and future Central Alaskan arcs, striking NW-SE along a >3,000 km trench. Further to the west, the new Farallon arc parallels the strike of the Alaskan (ANG) arcs over ~2,000 km length, sitting ~1,500 km south of them. On and close to the NAM margin, a long chain of older arcs is shutting down (Native & IMS), are overprinted, or transition southward into extensional volcanic fields (e.g. Saleeby and Dunne, 2015; Tosdal and Wooden, 2015; Busby and Centeno-García, 2022). NAM is exposed to westward pull because the seafloor west of it, which forms part of the NAM plate, is now subducting westward beneath the INS-GUE and Central Alaskan arcs (MEZ & ANG slabs). A rift zone between eastern NAM and west Africa transitions to full-blown westward drift by ~170 Ma, opening the Central Atlantic along a spreading ridge that is parallel to the INS-GUE trench.

Thus North America breaks away from Pangaea and is pulled into the Archipelago, with INS-GUE trench consuming the seafloor immediately west of NAM, the Mezcalera Ocean. Around ~150 Ma, NAM first collides with northern INS at conterminous U.S. latitudes (?northern California): at the easternmost point of the Archipelago, the Mezcalera Ocean has closed and collapsed into a suture. This continent-microcontinent collision deforms the margin locally (Nevadan orogeny), and the accreted (obducted) INS loads the continental margin, which develops topography that sheds sediments inland (Passage Beds of B.C. and Alberta) ~155 Ma. The collided segment of INS arc is extinguished.

NAM continues to be pulled into the Archipelago by the still-subducting segments of the Mezcalera and Angayucham Oceans, south and north of the collided segment. As NAM rides into the interior of the Archipelago, the seafloor sitting there is forced to subduct under the continental margin, i.e., eastward. In response a new arc is constructed above the lithosphere now subducting eastward beneath the continental margin. This is the SNB arc, the batholithic roots of which intrude and overprint the two older arcs: the accreted, extinct INS arc and the Native Triassic-Jurassic arc on stable NAM (extinct since ~170 Ma). The evolution of the override sequence and the three juxtaposed arcs are shown in Figure 8a.

NAM continues to be pulled west by the southern MEZ and by ANG subduction zones. They are trenches on a suicide mission: the continent collides with wider and wider (in latitude) swaths of INS-GUE arc segments, which go extinct and are replaced by SNB and allied arc forming above east subducting Farallon plate. From ~110 Ma, NAM also collides with future Central Alaskan arcs along ANG slab (Fig. 1). At latitudes of the CR (Fig. 1) ANG trench segments are not polarity-flipped due to the intervening Orcas micro-plate (Orcas basin in Fig. 1), which can slide out of the way rather than subduct.

Progressive accretion of arc segments intensifies the deformation of the margin and widens it in latitude into the Sevier and Columbian (in Canada) orogenies. Progressive closure of the Mezcalera Ocean between INS and NAM forms the collapsed basins of Figure 7, predicted by tomotectonics (Fig. 1) to have closed from ~150 Ma (in the U.S.) to ~100 Ma (in MX), as INS diachronously collided with NAM or with IMS (where IMS was pre-accreted to NAM).

Around 100 Ma, the Insular-Guerrero arc was extinct even in Mexico – the end of westward subduction at MX, US and southern BC latitudes. The Yukon margin and northern BC continued to be pulled into the Koyukuk arc. Farallon eastward subduction now reigned in the south: the SNB and allied arc on the margin (FS slab) had expanded south along the Mexican margin to form the Peninsular arc (Dickinson and Lawton, 2001). The northern Farallon arc (Pacific Rim terrane, and more) remained offshore, but by 90 Ma probably felt the approach of the NAM margin, now impinging on the Orcas microplate, which became substrate for both northern Farallon arc and the Koyukuk arc construction.

Around 80 Ma, the SNB arc on the margin suddenly shuts down (Big Break), probably related to disruption from initial override of the CR arc further north, and/or the collision of the Hess-Shatsky Rise conjugate plateau along FS trench (Livaccari et al., 1981; Humphreys, 2009; Humphreys et al., 2015, this volume). This sudden demise of the long-lived and margin-hugging FS trench decoupled the Sierra Nevada-Peninsular segment from the margin. The segment also included the accreted INS and IMS at U.S latitudes, then located north of the Sierra Nevada batholith. The Farallon plate transitions into transform motion (transpression) relative to NAM, and the transform boundary runs inside the soft continental lithosphere (speculatively mainly along the yellow line in Fig. 9a/b). The slivered-off parts of accreted INS and IMS ("Baja-BC") were free to move rapidly northward, as parts of the southern Farallon plate, and then as parts of the Orcas plate (Fig. 9b). Since the northern Farallon arc still sits offshore, Baja-BC can move north relatively unimpeded and *inboard* of the northern Farallon arc, assisted by the small, moveable Orcas microplate (as spelled out in section 6.2).

This transform corridor stays open for some tens of m.y. (recorded by disruption and retreat of upper CR slab), until by ~50 Ma the Orcas plate has gone, the northern Farallon trench has obliquely accreted to the Pacific Northwest margin, and established a new arc on the margin (Cascades arc). This margin-hugging new Farallon arc acts like a roadblock that ends the free passage of Baja-BC terranes.

The transform margin along the Sierra Nevada sector (San Andreas) continues to present, still slivering off continental fragments and transporting them north (Baja California, Salinian block, Transverse Ranges…) but only until they reach the impasse of the Juan de Fuca (northern Farallon) plate and its Cascades arc.

In the far north, the Koyukuk arcs that have been crumpling against the NAM margin (Fig. 9b, at 85 Ma), are further impacted by arrival of Baja-BC from the south, and Baja-BC gets wedged against the backstop of the Koyukuk arcs. As the Orcas microplate gets squeezed away or subducts, the INS and Central Alaskan arcs are compressed into the big terrane agglomerate that is Alaska (Fig. 9b).

Once the Koyukuk arc is completely extinct (ANG slab largely overridden by 50 Ma), the margin becomes turns transform. It remains a transform boundary to the present-day, still carrying parts of INS northward, albeit more slowly, at ~41 mm/yr (Leonard, et al., 2007).

6. Discussion

We first address the most common objections to the archipelago model. We then discuss the range of collision styles encountered (mainly ~150 to 80 Ma), followed by a discussion of margin-parallel translations ("Baja-BC", since ~80 to 50 Ma).

6.1 Objections to the archipelago model based on the nature of the Insular-Intermontane suture

Objections to the archipelago model (and the ~15 m.y. period of westward-only subduction at conterminous U.S. latitudes) have centered on supposedly discrepant geological characteristics of the Jura-Cretaceous suture between under-riding NAM and overriding Insular Superterrane.
Critics have pointed towards the lack of old detrital zircon sources in the archipelago, in order to explain the observed flooding of INS with old zircons, given that the Mezcalera Ocean originally (Fig. 6a) was of substantial width (1000-2000 km at its narrowest). Another criticism has concerned the lack of a persistent sedimentary basin on the leading edge of the subducting NAM plate.

Detrital zircons have been pointed to as a 'crucial test' of the archipelago model (LaMaskin et al., 2022). In this 'crucial test' zircons derived from cratonic NAM and the Native Triassic-Jurassic arc built upon its margin, should be absent in the overriding Insular Superterrane. Yet we have pointed to modern analogues for continent-beneath-arc collisional zones (Sigloch and Mihalynuk, 2017, 2019) where sediments derived from the continent and its margin are EXPECTED to be an increasingly predominant component during arc-continent convergence.
In modern examples of collision between continental margins and the arcs beneath which they subduct (Australia-Banda forming Timor, China-Luzon forming Taiwan), sediments containing zircons derived from the continent are observed on both the fore and back sides of the converging arc. Both Timor (e.g. Harris, 2011) and Taiwan (e.g. Beyssac et al., 2007) are comprised primarily of continentally-derived sediment, some of which transits the arc and is carried onto the overriding plate. Even isotopically primitive igneous rocks of the Luzon arc are overwhelmed by old, inherited zircons from the Chinese cratonic margin, prompting some workers propose an unexposed continental fragment underpinning the Luzon arc (Shao et al., 2015). In the case of the Insular Superterrane, objections based on lack of old zircons may be moot because basement of the superterrane itself includes possible sources of Early Paleozoic strata with abundant Precambrian zircons (e.g. Beranek et al, 2012; and noted, but discounted by LaMaskin et al., 2022). Hence the observed abundance of old continental zircons on INS does not

constitute a 'crucial test' against continent-beneath-arc collision, as proposed by LaMaskin et al. (2022); the modern-day analogues demonstrate quite the opposite.

Likewise, criticisms based on the lack of sediment load on the leading edge of the subducting continental plate are at odds with fundamental features of modern continent-beneath-arc collision zones. In both the Taiwan and Timor examples, amphibolite-grade metamorphic rocks are exhumed continentward of the colliding arc because the arc acts as a backstop for strata scraped off the subducting continental plate (fig. 8d). In the case of Taiwan, the subducting continental (China) margin is interpreted as a relict Andean-type arc (Cui et al., 2021), analogous to the extinct, Native-Jurassic arc that formed the leading edge of NAM in its collision with INS. Thus, the modern Luzon-China collision may be the best modern analogue for initial impingement of western NAM (California) with the Mezcalera arcs at ~155 Ma. A shortcoming of this analogy is the difference in the topography of the subducting plate. In the case of Taiwan, the eroded arc was older than 85 Ma when blanketed by Cenozoic sediments of the South China Sea, and the interface varies in depth by less than ~2400 m (Cui et al., 2021). In the North American case, only ~15 m.y. elapsed between cessation of active continental margin arc magmatism and collision of the archipelago (Sigloch and Mihalynuk, 2017, 2020), so rather than a broad submerged margin, one that had considerable relict topography is likely (e.g. Dickinson, 2018), and when deformed, produced confusing juxtapositions of basement and overlying strata.

We acknowledge that the creation of a plate model showing terrane motion paths and accurate relationships with other terranes while preserving recognizable terrane outlines is a challenge. With these constraints, our models (Henderson et al., 2014; Clennett et al., 2020) have not yet generated satisfactory motions for Klamath terranes (as pointed out by LaMaskin, et al., 2022), and this clearly requires future work. However, whether the Mezcalera suture lies between *bona fide* intra-oceanic arc of the Rogue-Chetco arc (Yule et al., 2006) bounded by the Orleans Fault, or includes arc, ophiolite, and mélange belts (e.g. Rattlesnake Creek terrane as used by Wyld and Wright, 1988) as far east as the North Fork terrane (as defined by Snoke and Barnes, 2006), does not alter the fundamental mantle underpinnings of the continental-scale suture between INS and NAM/IMS.

6.2 Double-sided subduction caused and shaped all collisions since 150 Ma

Much of the Archipelago debate has been framed in terms of eastward versus westward subduction. In reality, all arc collisions in the Archipelago were shaped by double-sided subduction, which defined the Archipelago from its inception (Fig. 6a). When the three major intra-oceanic arcs of MEZ, ANG and Farallon (CR, CR2) sprang into being all around the same time (at 1800-2000 km depth, corresponding to early Jurassic times), they reconfigured the eastern proto-Pacific from scratch. The earth favored double-sided subduction – with Farallon (CR, CR2) trenches pulling in lithosphere from the southwest, and directly facing off with ANG subduction, which sourced seafloor from the northeast. The CR and ANG trenches and slabs were parallel, with the Orcas microplate as a passive spacer between them. MEZ subduction, pulling in lithosphere from the east, worked in concert with ANG, although striking more obliquely to CR (fig. 6a). The "function" of this geometry is to permit two large ocean domains (Farallon Ocean and Mezcalera-Angayucham Ocean) to subduct simultaneously, in a configuration that could remain stable over long time scales, which presumably is an efficient mode of cooling the mantle. In support of this speculation of Archipelagoes as preferred modes of mantle convection, a close analogue to the Cordilleran Archipelago currently exists in the southwest Pacific (Sigloch & Mihalynuk, 2017). The Pacific Ocean and the Indian (formerly Tethys) Ocean subduct into this region from opposite sides without much mutual disruption. The interior of the archipelago – the region bounded by the Sunda arc, Papua-New Guinea, the Coral Sea arcs, and the Izu-Bonin and Mariana arcs –is complex in detail, with shifting configurations of minor trenches. Yet the basic functioning, of letting two big oceans subduct from the exterior, is robust. Slab walls are observed below the bounding trenches, indicating their stationarity (e.g., Hosseini et al., 2020).

6.2.1 Southern U.S. and Mexico: heads-on collision with subduction flip

In the first stage of Archipelago collisions, North America collided "only" with an eastward-protruding part of MEZ arc, while continuing to be pulled west by more southerly segments of MEZ and by all of ANG. It is crucial to not limit consideration of this collision along a singular 2-D cross section, as cartooned in Fig. 8a for 140 Ma, but also in and out of the plane (e.g., at Mexico and B.C. latitudes), where westward subduction kept pulling the NAM plate westward even after this direct trench pull had ceased at the point of collision on the U.S. margin ~155 Ma. Override of MEZ arc (INS and Guerrero superterranes) led to a gradual, orderly polarity flip along the collided segments, diachronous from northern California to Mexico. Intra-archipelago "southern Farallon" lithosphere (FS) was forced beneath the overridingcontinental margin, in the override sequence shown in Figures 1 and 5. A close analogue is the trench flip underway at the northern margin of Australia (Papua-New Guinea), which has breached the previously uninterrupted chains of Sunda and Coral Sea arcs and keeps getting pulled further northward by the surviving segments of those two arcs (Sigloch & Mihalynuk 2017).

The NAM-MEZ collision was thus succeeded by a sizable margin-hugging FS arc, along which the SNB and Peninsular batholiths coalesced, and beneath which was deposited an east-dipping slab (FS slab). However, FS slab is limited in space and time to this one discrete subduction episode from which Andean-style Farallon subduction has been extrapolated across the margin

The FS arc shut down suddenly, as recorded in the slabscape by the Big Break ~80 Ma (Fig. 1, yellow line). It is difficult to isolate specific causes in an interconnected plate-mantle system, but ultimately the SNB arc may have died because the motivating force, of slab pull into the Archipelago, diminished due to MEZ-ANG override. Arrival of the Hess-Shatsky plateau conjugate on the Farallon plate ~90 Ma, which was difficult to subduct (Livaccari et al. 1981), was likely another cause, or even the main cause, for the arc shutdown as FS subduction became flat beneath the continent, resisting the entry of more lithosphere. (Humphreys et al., 2015). In the tomotectonic interpretation, the plateau-arrival event is a transition of southern Farallon subduction from the regime of Figure 4F to 4H, caused by a strong decrease in sinking rate.

Given the lack of slab west of the Big Break, we interpret that the southwestern U.S. remained free of a continental arc after 80 Ma. The observed, spatially diffuse sweeps of "arc-like" magmatism across the western U.S. noted by various workers (see summary in Glazner, 2022) likely represent slab-window magmatism, when NAM lithosphere, continuing westward and pre-hydrated from below by the flat FS slab it had recently traversed, encountered the asthenosphere of the slab-free window. In absolute coordinates, the upper mantle region traversed by western NAM during the diffuse magmatic sweeps would have last been overlain by Baja-BC, which had however shuffled north most recently, events that may have further disturbed the upper mantle. While we cannot account for the spatial details of the magmatic sweep, we argue that the event looks unsurprising in the context of the region's upheaval, and that there is no compelling reason to interpret the sweep as "true" arc magmatism caused by subducting lithosphere. After the buoyant coupling of Farallon/Shatsky to NAM (~70 Ma), the continent's westward drift slowed by more than half for the next 40 m.y. (fig. 1).

6.2.2 Pacific Northwest, B.C., Alaska and "Baja-BC": 115-50 Ma collisions with double-sided subduction on the Orcas plate

In the late stage of arc collisions, NAM overrode the opposing ANG and CR trenches simultaneously and obliquely. ANG was overridden from ~115 Ma by North America moving parallel to the slab (Fig. 1, gold arrow), causing collisions at almost 90° angle with the ANG (Koyukuk) arcs, which had been welded into the Orcas microplate for as long as the archipelago existed, but which now crumpled into oroclines (terrane-wreck style; Johnston, 2008) to form the nucleus of Alaska.

The Orcas microplate was moveable due to its small size and seems to have diverted west- or northwestward when it felt the force of NAM approaching. This is recorded by the perturbed and westward-shallowing CR geometries of post-100 Ma times (green levels in Fig. 2), contrasting with the deeper, simple slab wall geometry of CR (red/yellow levels). Thus, the Orcas plate does not seem to have subducted under NAM, which it might have, analogous to the way that southern Farallon (FS) lithosphere started to subduct eastward after NAM had overridden MEZ arc (Fig. 8). Instead, the small Orcas plate was apparently squeezed out toward the (north)west. Ultimately, Orcas microplate had to subduct somewhere, and it may have quickly subducted into the small upper-mantle slab that strikes east-west under southern Saskatchewan, Alberta and B.C. (dark blue in Fig. 3a). This slab is not part of the sloping continuity of the northern Farallon group but rather seems to rest on top of it. Its location in Figure 9b is marked by the gray oval and two "??".

The Orcas microplate might be more aptly named "Alaska plate" because by 80 Ma, the components of future Alaska (except for Arctic Alaska), were all fringing this plate, as detailed by Figure 9b. They would be brought into contact and assembled by ~50 Ma, through the disappearance of the intervening Orcas lithosphere. Hence the northward "sprint" of Baja-BC must be a manifestation of the mobility and rapid demise of the Orcas plate during this squeeze phase. The northern Farallon (CR) arc could only make landfall on the continent (as Cascades continental trench since ~50 Ma) as and when the Orcas plate, into which the CR arc had always been welded (e.g., Pacific Rim terrane, now spread from Vancouver Island to southern Alaska), disappeared into the mantle.

We note that kinematically, the final demise stage (60-50 Ma) of the long-lived Orcas plate must be equated with the Cenozoic Resurrection plate (in an ironic mismatch of naming). This short-lived, Cenozoic microplate ordering B.C. and southern Alaska had been inferred from magmatic sweeps along the margin (Haeussler et al. 2003, Miller et al. 2023), and confirmed from upper-mantle geometries of the Farallon (FN) and Aleutian slabs by Fuston & Wu (2021).

6.2.3 Tomotectonic hypothesis testing on the three Sierra Nevada arcs

The field geologic record of the arc extinction / trench flip sequence is complex, because (at least) two arcs are produced in the same place (Fig. 8a). For MEZ, westward subduction ahead of the first-colliding margin segment (U.S. Sierra Nevada segment) was of decent duration, from MEZ/INS arc inception ~180 Ma(?) to first collision ~155 Ma. However, the geologic record of this INS arc is obscured by a later, overprinting arc, the Sierra Nevada Batholith arc (Fig. 8a, bottom). This overprinting is not an unlucky coincidence but an inevitable consequence of the arc collision / trench flip sequence. It is systematically predictable here and elsewhere (e.g., Papua-New Guinea or Taiwan).

Tomotectonics can help to frame geologic field studies and the generation of realistic hypotheses that guide predictive mapping. In the Sierra Nevada case above, the prediction would include a suture between a collapsed continental margin and outboard arc. Specifically the Calaveras mélange belt, the collapsed Mariposa basin that flanks it (Fig. 7), and that plutons produced by westward-subduction (INS) should be found only *outboard* of this Mezcalera Ocean suture. Following suturing, the later Sierra Nevadan arc magmatism could thermally overprint the suture and produce plutons both inboard and outboard of the suture.

Testing this hypothesis requires precise timing constraints, where the biggest challenge is to reliably distinguish plutons that are strictly of arc character (i.e., caused by mantle-wedge fluxing above the down-going Mezcalera plate and thus really recording the westward subduction episode), from plutons that are due to post-arc flare-up or to prograde or decompression remelting of older arc crust. On a continental arc margin (with abundant Native Triassic-Jurassic and Permian arc contributions) opportunities for confounding magmatic arc rock relationships are omnipresent (e.g. consider the Taiwan analogy, Fig. 8b)

Further confounding geologic relationships is the structural overprint during Baja-BC translation. For example, the north-south ordering of MEZ suture basins in Figure 7 is almost certainly not the same as their original north-south ordering, prior to translation. Our tomotectonic-constrained prediction would place the Sierra Nevada segment nearthe oldest MEZ suture (~155 Ma), and the Guerrero segment near the youngest MEZ suture (~110 Ma), with neither segment transported north to a significant degree. Locations that sutured between these original latitudinal limits of INS accretion are predicted intermediate suturing dates, but these basins have since been transported to British Columbia and southern Alaska. Hence, we cannot naively predict that northern basins should have older sutures than southern ones, even though that is what the override sequence of MEZ slab in Figure 1 would suggest. Baja-BC events must be restored before interpreting the older accretion record.

6.3 Tomotectonics infers BajaBC displacements, independent of paleomagnetism

"BajaBC" is a long-standing hypothesis developed to explain paleomagnetic measurements on Cordilleran terrestrial rocks, reproduced many times (Enkin 2006, Kent & Irving 2010), which indicate that Insular microcontinent and western parts of Intermontane microcontinent (Stikinia) originally accreted far south of their current locations, relative to NAM. Southern INS, now located in southern British Columbia, originally occupied Baja Californian (Mexican) latitudes (Irving 1985, Kent & Irving 2010). Alaskan parts of INS should accordingly have accreted at conterminous U.S. latitudes. The northward shuffle of 1500-2000 km happened between 80 Ma and ~50 Ma because rocks magnetized around 90 Ma show the full latitudinal offset, and rocks across most of British Columbia that were magnetized after 50 Ma show no significant offset relative to the North American craton. The 50 Ma to present history of northwest-most British Columbia and southern Alaska is much different. There, the evolving transform margin and its transition into the Aleutian arc accommodated significant northward offset from 50 Ma to present (see Hillhouse and Coe, 1994; Murphy, 2018).

INS constitutes the largest part of Baja-BC, and tomotectonic constraints require INS to have undergone large-scale northward displacement since its accretion, in an argument completely independent of rock magnetism. Figure 1 hindcasts that first accretion of INS to NAM at ~150 Ma occurred at conterminnos U.S. latitudes (northern California). This first collision involved northeastern promontory of MEZ slab, hence northern INS arc. Today, northernmost INS arc (Peninsular/Alexander terranes) is not abutting the conterminous U.S. but rather the southern Alaskan margin. Thus from tomotectonics arises the prediction that since its accretion, northern INS must have moved north relative to stable NAM, from conterminous U.S. latitudes to Alaskan latitudes. This amount of displacement is consistent with paleomagnetic data mainly from *southern* INS (southern B.C., Washington state), with an inferred original location at northern Mexican latitudes. Tomotectonics therefore provides remarkably straightforward support for paleomagnetic measurements that have still not gained widespread acceptance within the Cordilleran geoscience community.

Figure 9a shows the trajectories over time of the half dozen most robust paleomagnetic data sets that gave rise to the Baja-BC hypothesis. Data from many more sites support the timing of the northward sprint but are less robust. The blue/green trajectories follow the paleomagnetic sample sites back in time and space to where and when they were magnetized: Carmacks at 70 Ma, Churn Creek/Mount Tatlow at 95 Ma, 103 Ma for Spences Bridge, etc. (Enkin, 2006). All positions are given in absolute coordinates relative to the lower mantle. The Baja-BC sites are implemented to move northward rapidly between 70 Ma and 50 Ma. This timing is biased by paleomagnetic data; tomotectonic constraints permit translation any time between ~105 Ma (migration of the continental margin past ANG), and ~50 Ma (reestablishment of subduction leading to Cascade magmatism, evident by 45 Ma; Humphreys and Grunder, 2022).

The yellow line is our speculated location of the main Baja-BC transform fault ran. It is necessary to commit to a location when building a quantitative model like Clennett et al. (2020). We run the main Baja-BC shear inboard of all displaced sites of Figure 9a, but no more inboard than necessary (a conservative solution), and in locations that can plausibly hide a major fault. Mainly we run the fault through Intermontane terranes now located in B.C. and through presumed, left-behind IMS correlatives in the U.S. (in or west of the Blue Mountains; Mihalynuk & Diakow 2020, Tikoff et al. 2023).

In B.C., we speculate that the fault runs through the Cache Creek accretionary complex, sliding Stikinia past Quesnellia (as in Fig. 9b at 70 Ma). Displacement of Quesnellia is inferred to have been much less than Stikinia; however, paleomagnetic data on layered Mesozoic volcanic rocks of Quesnellia that are not compromised by resetting and pass all confidence tests, have yet to be obtained. Hence, we position the main Baja-BC shear zone conservatively between Quesnellia and Stikinia; in the intensely imbricated and poorly exposed Cache Creek terrane which separates them and could well hide this shear zone. In the Pacific Northwest U.S., its offset must be distributed somewhere between the dashed and the non-dashed line.

In California, we run the fault slightly outboard of the NAM-INS suture (identified with the Calaveras mélange belt and Mariposa collapsed basin in the Sierra Nevada; Fig. 7). The rationale is that not much of INS should be left in California if it is now found mainly in B.C. In practice, this means that we run the fault under the Central Valley, inspired by Wright and Wyld (2007), but we continue it *inboard* of the Klamaths, in order to implement ~1000 km northward translation of the Klamaths (Housen and Dorsey, 2005), past the stationary Sierra Nevada), which is recorded by Ochoco basin strata correlative with the Hornbrook Formation (Surpless and Beverly, 2013) that straddle the Klamath block (Housen, 2018). At the regional scales considered in this study, the uncertainties about the exact location of the fault(s) do not change any conclusions.

7. Conclusions and outlook

We have explained the tomotectonic method on a fully worked example for NAM. The method is based on a very simple, predictive, falsifiable null hypothesis, and a separation of geophysical (slab and plate tectonic) observations for making predictions, from geological observations for testing the predictions. The link between tomotectonics and geology is made by volcanic arcs above subducted paleo-lithosphere (slabs).

Since breaking away from Pangaea in early Jurassic times, North America has overridden a vast archipelago of intra-oceanic subduction zones and their arc terranes. This is supported by robust evidence in the mantle and at the surface. An archipelago is an oceanic area bounded by trenches that are oriented to pull in seafloor from opposite sides: a large-scale zone of plate convergence. All arc and microcontinent collisions of Cordilleran North America since ~150 Ma have been shaped by this double-sided nature of subduction. Different collision and deformation styles have occurred depending on the spacing of the two opposing trenches, and the angle at which North America collided with their arc terranes.

The accretion of Insular Superterrane, including the Sierra Nevada orogeny and arc succession was a case of subduction flip within the spacious interior of the archipelago. Oroclinal collapse of the Central Alaskan arcs against the continental margin, by westward subduction, was possible in the lee of the nearby, opposite-facing Farallon trench. The northward sprint of Baja-BC and its collapse against Central Alaska was a product of the same setting of closely spaced, opposing trenches.

Tomotectonics infers the large-scale northward displacement of Insular Superterrane (relative to stable North America) since it was accreted. This inference is completely independent of the paleomagnetic argument for Baja-BC, and supportive of it. A good understanding of these large-scale margin-parallel displacements between 80-50 Ma is crucial for the correct interpretation of the older accretions that pre-date Baja-BC, including the evidence for westward subduction. Slabs can be used to unscramble this record because they have stayed in their absolute paleo-positions, while surface elements have been much more mobile.

The tomotectonic null hypothesis, of subducted lithosphere sinking essentially vertically once it has entered its trench, is holding up so far. With very few degrees of freedom, the tomotectonic method capably predicts the known regional tectonic regimes (subduction, compression, transform) and their changes along various sectors of the NAM west coast from ~170 Ma to today. A useful contribution to tomotectonic hypothesis testing would be the development of tools for unequivocally discriminating igneous rocks formed in an arc above subducting lithosphere from similar magmatic rocks formed in other environments.

Acknowledgements

We thank Gene Humphreys and Terry Pavlis for their reviews, and Associate Editor Margi Rusmore for her additional comments and editorial handling, all of which helped to improve this manuscript.Editor Nancy Riggs and her team for the editorial handling. We are grateful to the organizers of the excellent Penrose conference that gave rise to this paper and volume: Stacia Gordon, Basil Tikoff, Elena Centeno-Garcia, William Matthews, and their organizing team. K.S. acknowledges funding by the European Research Council under the European Union's Horizon 2020 research and innovation program, grant 639003 DEEP TIME and by the French government through the UCAJEDI Investments in the Future project, reference number ANR-15-IDEX-01.
We dedicate this work to Eldridge Moores.

References

Atwater, T., 1970, Implications of plate tectonics for the Cenozoic tectonic evolution of western North America: Geological Society of America Bulletin, v. 81, p. 3513–3536.

Atwater, T., 1989, Plate tectonic history of the Northeast Pacific and western North America, in Winterer, E.L., Hussong, D.M., and Decker, R.W. eds., The eastern Pacific Ocean and Hawaii, Geological Society of America, Decade of North American Geology, v. N, p. 21–72.

Barth, A.P., Wooden, J.L., Jacobson, C.E. and Economos, R.C., 2013, Detrital zircon as a proxy for tracking the magmatic arc system: The California arc example. Geology, v. 41, p. 223-226.

Beyssac, O., Simoes, M., Avouac, J.P., Farley, K.A., Chen, Y.G., Chan, Y.C. and Goffé, B., 2007, Late Cenozoic metamorphic evolution and exhumation of Taiwan: Tectonics, v. 26, TC6001 [online]

Bunge, H.P., and Grand, S.P., 2000, Mesozoic plate-motion history below the northeast Pacific Ocean from seismic images of the subducted Farallon slab: Nature, v. 405, p. 337-340.

Busby, C.J., and Centeno-García, E., 2022, The "Nazas Arc" is a continental rift province: implications for Mesozoic tectonic reconstructions of the southwest Cordillera, US and Mexico: Geosphere, 18, p. 647-669.

Busby, R.W., and Aderhold, K., 2020, The Alaska transportable array: As built. Seismological Research Letters, v. 91, p.3017-3027.

Canil, D., and Morris, R.A., 2024, Continentalization of an intraoceanic arc as exemplified by the Jurassic Bonanza arc of Vancouver Island, Canada: Geological Society of America Bulletin, v. 136, p. 880-892.

Cerpa, N.G., Sigloch, K., Garel, F., Heuret, A., Davies, D.R., and Mihalynuk, M.G., 2022, The effect of a weak asthenospheric layer on surface kinematics, subduction dynamics and slab morphology in the lower mantle: Journal of Geophysical Research: Solid Earth, v. 127, p. e2022JB024494.

Chapman, A.D., Saleeby, J.B., Wood, D.J., Piasecki, A., Kidder, S., Ducea, M.N., and Farley, K.A., 2012, Late Cretaceous gravitational collapse of the southern Sierra Nevada batholith, California: Geosphere, v. 8, p. 314-341.

Clennett, E.J., Sigloch, K., Mihalynuk, M.G., Seton, M., Henderson, M.A., Hosseini, K., Mohammadzaheri, A., Johnston, S.T., and Müller, R.D., 2020, A quantitative tomotectonic plate reconstruction of western North America and the eastern Pacific basin: Geochemistry, Geophysics, Geosystems, v. 21, p.e2020GC009117.

Clowes, R.M., Brandon, M.T., Green, A.G., Yorath, C.J., Brown, A.S., Kanasewich, E.R., and Spencer, C., 1987, LITHOPROBE-southern Vancouver Island: Cenozoic subduction complex imaged by deep seismic reflections: Canadian Journal of Earth Sciences, v. 24, p. 31–51.

Cowan, D.S., 2003, Revisiting the Baranof-Leech River hypothesis for early Tertiary coastwise transport of the Chugach-Prince William Terrane: Earth and Planetary Science Letters, v. 213, p. 463–475, doi: 10.1016/s0012-821x(03)00300-5.

Cowan, D.S., Brandon, M.T., and Garver, J.I., 1997, Geological tests of hypotheses for large coastwise displacements; a critique illustrated by the Baja British Columbia controversy: American Journal of Science, v. 297, p. 117-173.

Cui, Y., Shao, L., Li, Z.X., Zhu, W., Qiao, P., and Zhang, X., 2021, A Mesozoic Andean-type active continental margin along coastal South China: New geological records from the basement of the northern South China Sea. Gondwana Research, v. 99, p. 36-52.

Dickinson, W.R., 2008, Accretionary Mesozoic-Cenozoic expansion of the Cordilleran continental margin in California and adjacent Oregon: Geosphere, v. 4, p. 329–353, doi: 10.1130/GES00105.1.

Dickinson, W.R., 2018, Tectonosedimentary Relations of Pennsylvanian to Jurassic Strata on the Colorado Plateau: Geological Society of America Special Paper 533, 184 p., https://dx.doi.org/10.1130/2018.2533.

Dickinson, W.R., and Lawton, T.F., 2001, Carboniferous to Cretaceous assembly and fragmentation of Mexico: Geological Society of America Bulletin, v. 113, p. 1142–1160.

du Bray, E.A., John, D.A., and Cousens, B.L., 2014, Petrologic, tectonic, and metallogenic evolution of the southern segment of the ancestral Cascades magmatic arc, California and Nevada: Geosphere, v. 10, p. 1-39.

Dumitru, T.A., Wakabayashi, J., Wright, J.E., and Wooden, J.L., 2010, Early Cretaceous transition from nonaccretionary behavior to strongly accretionary behavior within the Franciscan subduction complex: Tectonics, v. 29, http://onlinelibrary.wiley.com/doi/10.1029/2009TC002542/full.

Earth Model Collaboration, 2024, A repository of Earth models providing the NSF SAGE and GAGE research community model preview visualization tools, facilities to extract model data/metadata, and access to the contributed processing software, URL: Earth Model Collaboration / EarthScope Consortium | Observable (observablehq.com) [accessed July, 2024].

Engebretson, D.C., Cox, A., and Gordon, R.G., 1985, Relative motions between oceanic and continental plates in the Pacific basin: Geological Society of America Special Paper 206, p. 1–60.

Enkin, R.J., 2006, Paleomagnetism and the case for Baja British Columbia: Paleogeography of the North American Cordillera, in Haggart, J. Enkin, R.J. and Monger, J.W.H., eds., Paleogeography of the North American Cordillera, Evidence For and Against Large-Scale Displacements: Geological Association of Canada Special Paper 46, p. 233–253.

Forsyth, D., and Uyeda, S., 1975, On the relative importance of the driving forces of plate motion: Geophysical Journal International, 43, p. 163-200.

Fu, R.R., and Kent, D.V., 2018, Anomalous Late Jurassic motion of the Pacific Plate with implications for true polar wander: Earth and Planetary Science Letters, v. 490, p. 20-30.

Fuston, S. L., 2022, Reconciling North American Tectonics with the Deep Mantle through Structurally Unfolding Subducted Slabs and Mantle Convection Modeling: Ph.D. thesis, University of Houston, 115 p.

Fuston, S., and Wu, J., 2021, Raising the Resurrection plate from an unfolded-slab plate tectonic reconstruction of northwestern North America since early Cenozoic time: GSA Bulletin, v. 133, p. 1128-1140.

Garver, J.I., and Davidson, C.M., 2015, Southwestern Laurentian zircons in upper Cretaceous flysch of the Chugach-Prince William terrane in Alaska: American Journal of Science, v. 315, p. 537-556.

Glazner, A.F., 2022, Cenozoic magmatism and plate tectonics in western North America: Have we got it wrong?, in Foulger, G.R., Hamilton, L.C., Jurdy, D.M., Stein, C.A., Howard, K.A., and Stein, S., eds., In the Footsteps of Warren B. Hamilton: New Ideas in Earth Science: Geological Society of America Special Paper 553, p. 1–14, https://doi.org/10.1130/2021.2553(09).

Gorbatov, A., Widiyantoro, S., Fukao, Y., and Gordeev, E., 2000, Signature of remnant slabs in the North Pacific from P-wave tomography: Geophysical Journal International, v. 142, p. 27-36.

Haeussler, P. J., Bradley, D. C., Wells, R. E., and Miller, M. L., 2003, Life and death of the Resurrection plate: Evidence for its existence and subduction in the northeastern Pacific in Paleocene–Eocene time: Geological Society of America Bulletin, v. 115, p. 867-880.

Harris, R., 2011, The nature of the Banda Arc–continent collision in the Timor region, in Brown, D., and Ryan, P.D., eds., Arc-continent collision: Springer, pp. 163-211.

Hess, H. H., 1965, Mid-Oceanic Ridges and Tectonics of the Sea-Floor, in Whittard, W.F., and Bradshaw, R., eds., Submarine Geology and Geophysics: Proc. 17th Symposium of the Colston Research Society, 5-9 April 1965, Bristol, p. 317-332.

Hildebrand, R.S., 2009, Did Westward Subduction Cause Cretaceous–Tertiary Orogeny in the North American Cordillera?: Geological Society of America Special Paper 457, 71 p., https://doi.org/10.1130/SPE457. Hildebrand, R.S., 2013, Mesozoic assembly of the North American Cordillera: Geological Society of America Special Paper 495, 169 p.

Hillhouse, J. W., and Coe, R. S., 1994, Paleomagnetic data from Alaska, in Plafker, G., and Berg, H. C., eds., The Geology of Alaska: Boulder, Colorado, Geological Society of America, The Geology of North America, v. G-l, p. 797-812

Hosseini, K., and Sigloch, K., 2015, Multifrequency measurements of core-diffracted P waves (Pdiff) for global waveform tomography: Geophysical Journal International, v. 203, p. 506–521.

Hosseini, K., Matthews, K.J., Sigloch, K., Shephard, G.E., Domeier, M., and Tsekhmistrenko, M., 2018, SubMachine: Web-based tools for exploring seismic tomography and other models of Earth's deep interior: Geochemistry, Geophysics, Geosystems, v. 19, p. 1464-1483.

Hosseini, K., Sigloch, K., Tsekhmistrenko, M., Zaheri, A., Nissen-Meyer, T., and Igel, H., 2020, Global mantle structure from multifrequency tomography using P, PP and P-diffracted waves: Geophysical Journal International, v. 220, p.96-141.

Housen, B.A., and Dorsey, R.J., 2005, Paleomagnetism and tectonic significance of Albian and Cenomanian turbidites, Ochoco basin, Mitchell Inlier, central Oregon: Journal of Geophysical Research: Solid Earth, v. 110, p. 1-22, doi:10.1029/2004JB003458.

Humphreys, E., 2009, Relation of flat subduction to magmatism and deformation in the western United States, in Kay, S.M., Ramos, V.A., and Dickinson, W.R., eds., Backbone of the Americas: Shallow Subduction, Plateau Uplift, and Ridge and Terrane Collision: Geological Society of America Memoir 204, p. 85-98, doi: 10.1130/2009.1204(04)

Humphreys, E.D., and Grunder, A.L., 2022, Tectonic controls on the origin and segmentation of the Cascade Arc, USA: Bulletin of Volcanology, v. 84, p.102.

Humphreys, E.D., Schmandt, B., Bezada, M.J., and Perry-Houts, J., 2015, Recent craton growth by slab stacking beneath Wyoming: Earth and Planetary Science Letters, v. 429, p. 170–180, doi: 10 .1016 /j .epsl .2015 .07 .066 .Müller, R.D., Sdrolias, M., Gaina, C., and Roest, W.R., 2008, Age, spreading rates, and spreading asymmetry of the world's ocean crust: Geochemistry, Geophysics, Geosystems – G3, v. 9, doi: 10.1029/2007GC001743.

Humphreys, E.D., Clennett, E.J., Wu, J., and van Buer, N.J., 2024, Reconciling Baja-BC and flat Shatsky conjugate subduction beneath the western U.S. THIS VOLUME.

Irving, E., 1985, Whence British Columbia: Nature, v. 314, p. 673-674.

Jicha, B.R., and Kay, S.M., 2018, Quantifying arc migration and the role of forearc subduction erosion in the central Aleutians: Journal of Volcanology and Geothermal Research, v. 360, p. 84-99.

Johnston, S.T., 2008, The Cordilleran ribbon continent of North America: Annual Review of Earth and Planetary Sciences, v. 36, p. 495–530, doi: 10.1146/annurev.earth.36.031207.124331.

Johnston, S.T., 2001, The Great Alaskan Terrane Wreck: reconciliation of paleomagnetic and geological data in the northern Cordillera: Earth and Planetary Science Letters, v. 193, p. 259–272.

Kent, D.V., and Irving, E., 2010, Influence of inclination error in sedimentary rocks on the Triassic and Jurassic apparent pole wander path for North America and implications for Cordilleran tectonics: Journal of Geophysical Research B, Solid Earth, v. 115, p. 1-25, doi: 10.1029/2009JB007205.

Leonard, L.J., Hyndman, R.D., Mazzotti, S., Nykolaishen, L., Schmidt, M., and Hippchen, S., 2007, Current deformation in the northern Canadian Cordillera inferred from GPS measurements: Journal of Geophysical Research: Solid Earth, v. 112, p. 1-15, B11401, doi:10.1029/2007JB005061

Livaccari, R. F., Burke, K., and Sengor, A. M. C., 1981, Was the Laramide orogeny related to subduction of an oceanic plateau?: Nature, v. 289, p. 276–278.

Lithgow-Bertelloni, C., and Richards, M. A., 1998, The dynamics of Cenozoic and Mesozoic plate motions: Reviews of Geophysics, v. 36, p. 27-78.

Liu, L., Spasojevic, S., & Gurnis, M. (2008). Reconstructing Farallon plate subduction beneath North America back to the Late Cretaceous. Science, 322(5903), 934-938.

Meltzer, Anne, et al., 1999, The USArray initiative: Geological Society of America Today v. 9, p. 8-10.

Mihalynuk, M.G., and Diakow, L.J., 2020, Southern Nicola arc geology. British Columbia Ministry of Energy, Mines and Low Carbon Innovation, British Columbia Geological Survey Geoscience Map 2020-01, 1:50,000 scale, two sheets.

Mihalynuk, M.G., Erdmer, P., Ghent, E.D., Cordey, F., Archibald, D.A., Friedman, R.M., and Johannson, G.G., 2004, Coherent French Range blueschist: Subduction to exhumation in < 2.5 m.y.?: Geological Society of America Bulletin, v. 116, p. 910–922, doi: 10.1130/b25393.

Miller, R. B., Umhoefer, P. J., Eddy, M. P., and Tepper, J. H., 2023, Upper-plate response to ridge subduction and oceanic plateau accretion, Washington Cascades and surrounding region: Implications for plate tectonic evolution of the Pacific Northwest (USA and southwestern Canada) in the Paleogene: Geosphere, v. 19, p. 1157-1179.

Monger, J.W., and Gibson, H.D., 2019, Mesozoic-Cenozoic deformation in the Canadian Cordillera: The record of a "Continental bulldozer"?: Tectonophysics, v. 757, p.153-169.

Moores, E.M., 1970, Ultramafics and orogeny, with models of the US Cordillera and the Tethys: Nature, v. 228, p. 837–842.

Moores, E.M., 1998, Ophiolites, the Sierra Nevada, "Cordilleria," and orogeny along the Pacific and Caribbean margins of North and South America: International Geology Review, v. 40, p. 40–54.

Morgan, W. J., 1968, Rises, trenches, great faults, and crustal blocks: Journal of Geophysical Research, v. 73, p. 1959-1982.

Morgan, W.J., 1983, Hotspot tracks and the early rifting of the Atlantic: Developments in Geotectonics, v. 19, p. 123-139).

Müller, R. D., Roest, W. R., and Royer, J. Y., 1998, Asymmetric sea-floor spreading caused by ridge–plume interactions: Nature, v. 396, p. 455-459.

Müller, R.D., Sdrolias, M., Gaina, C., and Roest, W.R., 2008, Age, spreading rates, and spreading asymmetry of the world's ocean crust: Geochemistry, Geophysics, Geosystems – G3, v. 9, doi: 10.1029/2007GC001743.

Murphy, D.C., 2018, Latest Cretaceous–early Eocene Pacifi c-Arctic?-Atlantic connection: Co-evolution of strike-slip fault systems, oroclines, and transverse fold and-thrust belts in the northwestern North American Cordillera, in Piepjohn, K., Strauss, J.V., Reinhardt, L., and McClelland, W.C., eds., Circum-Arctic Structural Events: Tectonic Evolution of the Arctic Margins and Trans-Arctic Links with Adjacent Orogens: Geological Society of America Special Paper 541, p. 1–22, https://doi.org/10.1130/2018.2541(28).

O'Neill, C., Mueller, D., and Steinberger, B., 2005, On the uncertainties in hot spot reconstructions and the significance of moving hot spot reference frames: Geochemistry, Geophysics, Geosystems – G3, v. 6, doi: 10.1029/2004GC000784.

Paterson, S.R., and Ducea, M.N., 2015, Arc magmatic tempos: Gathering the evidence: Elements, v. 11, p. 91-98.

Patton Jr, W.W., and Box, S.E., 1989, Tectonic setting of the Yukon-Koyukuk basin and its borderlands, western Alaska: Journal of Geophysical Research: Solid Earth, v. 94, p. 15807-15820.8, DOI: 10.2113/gselements.11.2.91

Pavlis, G.L., Sigloch, K., Burdick, S., Fouch, M.J., and Vernon, F.L., 2012, Unraveling the geometry of the Farallon plate: Synthesis of three-dimensional imaging results from USArray: Tectonophysics, v. 532–535, p. 82–102, doi: 10 .1016 /j .tecto .2012 .02 .008 .

Pavlis, T.L., Amato, J.M., Trop, J.M., Ridgway, K.D., Roeske, S.M., and Gehrels, G.E., 2019, Subduction polarity in ancient arcs: A call to integrate geology and geophysics to decipher the Mesozoic tectonic history of the Northern Cordillera of North America: GSA Today, v. 29, p. 4-10.

Ribe, N.M., Stutzmann, E., Ren, Y., and van der Hilst, R., 2007, Buckling instabilities of subducted lithosphere beneath the transition zone: Earth and Planetary Science Letters, v. 254, p. 173–179, doi: 10.1016/j.epsl.2006.11.028.

Saleeby, J., and Dunne, G., 2015, Temporal and tectonic relations of early Mesozoic arc magmatism, southern Sierra Nevada, California, in Anderson, T.H., Didenko, A.N., Johnson, C.L., Khanchuk, A.I., and MacDonald, J.H., Jr., eds., Late Jurassic Margin of Laurasia—A Record of Faulting Accommodating Plate Rotation: Geological Society of America Special Paper 513, p. 223–268, doi:10.1130/2015.2513(05).

Schweickert, R.A., 2015, Jurassic evolution of the Western Sierra Nevada metamorphic province, in Anderson, T.H., Didenko, A.N., Johnson, C.L., Khanchuk, A.I., and MacDonald, J.H., Jr., eds., Late Jurassic Margin of Laurasia—A Record of Faulting Accommodating Plate Rotation: Geological Society of America Special Paper 513, p. 299–358, doi:10.1130/2015.2513(08).

Seton, M., Müller, R.D., Zahirovic, S., Gaina, C., Torsvik, T., Shephard, G., Talsma, A., Gurnis, M., Turner, M., Maus, S., and Chandler, M., 2012, Global continental and ocean basin reconstructions since 200 Ma: Earth-Science Reviews, v. 113, p. 212–270, doi: 10.1016/j.earscirev.2012.03.002.

Sigloch, K., 2008, Multiple-Frequency Body-Wave Tomography [Ph.D. thesis]: Princeton, New Jersey, Princeton University, 249 p.

Sigloch, K., 2011, Mantle provinces under North America from multifrequency P-wave tomography: Geochemistry Geophysics Geosystems, v. 12, Q02W08, doi: 10.1029 /2010GC003421 .

Sigloch, K., and Mihalynuk, M.G., 2013, Intra-oceanic subduction shaped the assembly of Cordilleran North America: Nature, v. 496, p. 50–56, doi: 10 .1038/nature12019 .

Sigloch, K., and Mihalynuk, M.G., 2020, Comment on GSA Today article by Pavlis et al., 2019: "Subduction polarity in ancient arcs: A call to integrate geology and geophysics to decipher the Mesozoic tectonic history of the northern Cordillera of North America": GSA Today, v. 30, p. e47-e50, https://doi.org/10.1130/GSATG431C.1.

Sigloch, K., McQuarrie, N., and Nolet, G., 2008, Two-stage subduction history under North America inferred from multiple-frequency tomography: Nature Geoscience, v. 1, p. 458–462, doi: 10 .1038 /ngeo231.

Stegman, D. R., Farrington, R., Capitanio, F. A., and Schellart, W. P., 2010, A regime diagram for subduction styles from 3-D numerical models of free subduction: Tectonophysics, v. 483, p. 29-45.

Steinberger, B., Torsvik, T. H., and Becker, T. W., 2012, Subduction to the lower mantle–a comparison between geodynamic and tomographic models: Solid Earth, v. 3, p. 415-432.

Surpless, K.D., and Beverly, E.J., 2013, Understanding a critical basinal link in Cretaceous Cordilleran paleogeography: Detailed provenance of the Hornbrook Formation, Oregon and California: GSA Bulletin, v. 125, p. 709-727.

Tardy, M., Lopierre, H., Bourdier, J.L., Coulon, C., Hernández, L.E.O., and Yta, M., 1992, Intraoceanic setting of the western Mexico Guerrero terrane--implications for the Pacific-Tethys geodynamic relationships during the Cretaceous: Revista mexicana de ciencias geológicas, v. 10, p. 118-128.

Tepper, J.H., and Clark, K.P., 2024, Initiation of the Cascade arc: Geology, v. 52, p. 297–301, https://doi.org/10.1130/G51888.1

Tikoff, B., Housen, B.A., Maxson, J.A., Nelson, E.M., Trevino, S., and Shipley, T.F., 2023, Hit-and-run model for Cretaceous–Paleogene tectonism along the western margin of Laurentia, in Whitmeyer, S.J., Williams, M.L., Kellett, D.A., and Tikoff, B., eds., Laurentia: Turning Points in the Evolution of a Continent: Geological Society of America Memoir 220, p. 659–705, https://doi.org/10.1130/2022.1220(32).

Tomek, F., Žák, J., Verner, K., Ježek, J., and Paterson, S.R., 2024, A complex interplay between pluton emplacement, tectonic deformation, and plate kinematics in the Cretaceous Sierra Nevada magmatic arc, California: Tectonics, v. 43, p. e2023TC007822.

Torsvik, T.H., Steinberger, B., Shephard, G.E., Doubrovine, P.V., Gaina, C., Domeier, M., Conrad, C.P., and Sager, W.W., 2019, Pacific‐Panthalassic reconstructions: Overview, errata and the way forward: Geochemistry, Geophysics, Geosystems, v. 20, p. 3659-3689.

Tosdal, R.M., and Wooden, J.L., 2015, Construction of the Jurassic magmatic arc, southeast California and southwest Arizona, in Anderson, T.H., Didenko, A.N., Johnson, C.L., Khanchuk, A.I., and MacDonald, J.H., Jr., eds., Late Jurassic Margin of Laurasia—A Record of Faulting Accommodating Plate Rotation: Geological Society of America Special Paper 513, p. 189–221, doi:10.1130/2015.2513(04).

Van der Meer, D.G., Van Hinsbergen, D.J., and Spakman, W., 2018, Atlas of the underworld: Slab remnants in the mantle, their sinking history, and a new outlook on lower mantle viscosity: Tectonophysics, v. 723, p. 309-448.

van der Wiel, E., van Hinsbergen, D. J., Thieulot, C., and Spakman, W., 2024, Linking rates of slab sinking to long-term lower mantle flow and mixing: Earth and Planetary Science Letters, v. 625, 118471.

Wessel, P., and Kroenke, L.W., 2008, Pacific absolute plate motion since 145 Ma: An assessment of the fixed hot spot hypothesis: Journal of Geophysical Research: Solid Earth, v. 113, B06101, , 21 p.

Wright, J.E., and Wyld, S.J., 2007, Alternative tectonic model for Late Jurassic through Early Cretaceous evolution of the Great Valley Group, California, in Cloos, M., Carlson, W.D., Gilbert, M.C., Liou, J.G., and Sorensen, S.S., eds., Convergent Margin Terranes and Associated Regions: A Tribute to W.G. Ernst: Geological Society of America Special Paper 419, p. 81-96.

Figure captions

Figure 1. Roadmap figure for this study: the superposition of subducted lithosphere (slabs) in the mantle with continental drift, reconstructed with respect to the mantle. Coloured polygons show outlines of major slabs under North America from teleseismic P-wave tomography (Sigloch 2011). Slabs inferred to have been deposited by westward subduction are coloured in orange, those generated by eastward (Farallon) subduction in green. Darker colour shades are applied to lower-mantle slabs (MEZ, ANG and CR/CR2/W; light shades to shallower slabs: FS (400-1000 km deep), FN (0-700 km), and to the shallow western end of ANG. Superimposed are time snapshots tracking the westward migrating margin of North America, reconstructed in a mantle reference frame, which is constrained between 0-120 Ma by moving hotspots (Dubrovine et al., 2012) and 120-170 Ma by true polar wander-corrected paleomagnetic data (Torsvik et al., 2019). Colored arrows connecting the northern end points of the paleo-coastlines highlight three distinct episodes of absolute plate motion.
If the slabs sank vertically in place then a continental margin overlying a slab indicates a continent-arc interaction – because a slab constrains a paleo-subduction zone, which must have hosted a paleo-arc. Symbols on the paleo-margins indicate the nature of the tectonic regime along the margin, as inferable from the tomotectonic principles developed in the text. Orange barbs: NAM-beneath-arc collision (westward subducting slab located underneath). Green barbs: subduction beneath NAM (eastward subduction), with arc built on NAM. Light blue lines and arrows: transform boundary along the margin (no slab underneath). Black line: (quasi-)passive continental margin (no slab underneath, and no pre-existing plate boundary along the margin). Yellow line traces the sharp western edge of FS slab, associated with a sudden transition from eastward subduction to transform margin ~80 Ma. The starting point of our inference is ~170 Ma, the time when North America separated from Pangaea, and when absolute paleo-positioning in plate reconstructions becomes reasonably reliable.
Slab abbreviations: MEZ – Mezcalera, ANG – Angayucham, CR & CR2 – Cascadia Root, FN – Farallon North, FS – Farallon South. W is a non-interpretive slab name.

Figure 2. Mantle tomography: 3-D isosurface rendering of seismically fast anomalies imaged under the western U.S.A., from the surface to ~1800 km depth, in the teleseismic P-wave tomography model of Sigloch (2011). The isosurface rendering threshold is $dVp/Vp>0.25\%$. Color signals depth and changes in increments of 200 km. This structure represents subducted oceanic lithosphere (slab) of the former Farallon plate, dipping eastward down from beneath the Cascades (Juan de Fuca) trench. Surface topography of the North American Cordillera and the Pacific basin are overlain in translucent gray, with strong vertical exaggeration. Yellowstone (red triangle) and its vertical downward continuation are shown for visual reference. Seismically slow anomalies are not rendered (e.g., Yellowstone plume). Shallow fast anomalies representing the thick continental lithosphere of NAM are masked out as they would block the 3-D view on the slabscape. Panels A and B present alternative view angles on the same scene, comprising the FN and CR slabs of Figure 1 (subdivided at ~600 km depth, where structural breaks are visible especially in panel B). Slab W is also visible in the foreground. Deep CR2 slab under the Pacific is not rendered.

Figure 3. Three-dimensional isosurface rendering of all seismically fast P-wave anomalies (subducted slabs) in the upper and lower mantle beneath North America. Tomography model, rendering threshold and color scheme as in Figure 2. (A) Top-down view of fast structure below 400 km (in order to exclude

the overlying lithosphere, which is fast but does not represent slab). Strictly speaking, the view is from ~390 km down due to slight interpolation smoothing of the contouring algorithm, explaining why the shallowest anomalies appear in dark blue, as part of the 200-400 km layer. (B) Inside-out view of all fast structure from the surface down, with the deepest structure (slab walls MEZ, ANG, CR/CR2) emerging to the foreground. Imaging limitations include artifacts, especially near the margins of the regional dataset: resolution lost into the ocean basins and north of 55°. Two downward smearing artifacts are labeled with white x's and are not interpreted.

Figure 4. (A) The tomotectonic null hypothesis of vertical slab sinking, as envisioned by the very first cartoon of subduction to be published, by Harry Hess in 1965. Motions are drawn in a mantle reference frame, with the overriding plate moving laterally but not the subducting plate. (B)-(I) Range of possible slab geometries predicted for when oceanic lithosphere sinks vertically after entering the trench, as a function of the parameters v_o, the velocity of the overriding plate (or arc) on the x-axis, and of K, a measure for the vigor of subduction, on the y-axis. Dashed lines represent the viscosity discontinuity between upper mantle (UM) and lower mantle (LM), where the mantle becomes 1-2 orders of magnitude more viscous, resisting further slab sinking. Motions are drawn relative to the mantle, and velocity arrows are drawn to scale relative to each other. v_z, the slab sinking velocity in the lower mantle, is kept fixed in all panels (a typical value being 10 mm/year). Kinematic ratio $K = v_{sub}/v_{acc}$ is the ratio of slab length subducted per unit time versus the length of accommodation space created for it, by means of the vertical sinking away of older slab and the migration v_o of the trench away from the site of older subduction (see Cerpa et al. 2022, eq. 1, for exact definition). K>1 indicates "traffic jam conditions", where plate convergence is too rapid to be accommodated undeformed, so that slab is forced to thicken (probably by folding). The average value observed for present-day trenches is K~2.5 (Cerpa et al. 2022), with the associated slab types highlighted by grey shaded panels D, F, H. $v_o < 0$ (trench advance, panels B & C) is practically not observed.

Figure 5. Paleo-trenches in absolute (mantle) coordinates, as predicted by the observed slab geometries of Figure 3 if the slabs sank vertically. Slab-to-trench transcriptions are drawn in depth increments of 100 km, using the same depth-to-colour mapping as Figure 3. Tracks of paleo-trench (or arc) locations are shown as thick lines if inferred to be produced by westward subduction, and thin lines if produced by eastward subduction or subduction of ambiguous polarity (mostly Farallon). For laterally extended slabs (FS, FN, CR, presumably produced as in figs 4F/H), the arc lines are shown as dashed when a locus of slab deposition is poorly constrained laterally, for a given depth. The colour bar also shows an indicative mapping of slab depth to time of subduction, using 10 mm/year as a typical, heuristic value for slab sinking rate. The coastlines of NAM reconstructed at times 170 Ma (black), ~80 Ma (green), and present day (grey). Grey polygons indicate slab footprints at 800 km depth (in light grey) and at 1400 km (dark grey). Label SN marks the approximate position of the Sierra Nevada batholith; the arrow denotes possible extents of the Hess-Shatsky Rise conjugate plateau. Arc abbreviations: A = Aleutian, KI = Kula-Izanagi. Purple-grey stars on western NAM mark the previous generation of arcs IMS & NJ, extinct and accreted by 170 Ma.

Figure 6. Tomotectonic constraints on the growth and consumption of ocean basins subducting into the Archipelago from opposite sides. (A) Time frame for 170 Ma (early Archipelago before NAM started moving west) and (B) for 80 Ma (override far advanced, westward subduction almost overridden). Trenches/arcs active at the respective reconstruction times are highlighted with barbs and the colours corresponding to their depths, and are plotted on the basemap of Figure 4, which shows all arc tracks

over time. In (A), the lateral gap between the NAM and its nearest slabs (MEZ, ANG) constrains the extents of a paleo-ocean at 170 Ma (the Mezcalera-Angayucham Ocean), whose westward subduction into MEZ/ANG allows NAM to advance westward. The lateral gap between the reconstructed Farallon spreading ridge (isochrons preserved on today's Pacific plate) and its nearest slabs (CR, CR2) constraints the extents of another paleo-ocean, the Farallon Ocean. Orcas Basin is an oceanic microplate inferred to occupy the space between the double-sided, intra-oceanic CR and ANG trenches. (B) By 80 Ma, lateral overlap of NAM with arc tracks indicates accomplished arc collisions and accretions, except in the far northwest of the ANG arc. Lateral overlap of NAM with the FS slab indicates that the (southern) Farallon trench is flush against the continental margin. The enduring gap between NAM and the CR slab further north indicates that the northern Farallon arc continues to sit offshore (but is in the process of being overridden and converted into a marginal arc, the future Cascades arc).

Figure 7. Arc terranes matched to slabs. Every substantive slab should be associated with a geologically known arc, and every known arc should be associated with a slab. Arc (super-)terranes are shown in their present positions in the Cordillera on the left part of the map. The same arc terranes are schematically reconstructed above their matched slabs and paleo-trenches, in absolute positions relative to the lower mantle. Colour legend gives the interpreted matches of slabs to geologically known arcs. Superterranes, slabs, arcs and trenches are coloured green if associated with Farallon Ocean subduction; orange if associated with Mezcalera Ocean subduction, and red if associated with Angayucham Ocean subduction. The reconstruction time for the arcs and slab walls corresponds to ~170 Ma (before Archipelago override began), except in the case of the SW-ward migrating southern Farallon (Sierra Nevada Batholith) arc, which is shown in several time snapshots migrating across the area occupied by its associated FS slab. North America is reconstructed at 170 Ma, 140 Ma and 0 Ma. Intermontane Superterrane (IMS) and its continental prolongation, the Native Jurassic arc (NJ) are coloured purple; by 170 Ma, their arc activity had ceased and IMS is shown docked against NAM. The interpreted suture of MEZ arcs (Insular & Guerrero Superterranes INS, orange) against IMS/NJ terranes, is represented by a dozen of collapsed oceanic basins coloured cyan and numbered/labeled in the legend.

Abbreviations: Guerrero-Insular arc terranes include WR (Wrangellia), AX (Alexander), PE (Peninsular), GU (Guerrero), WF (Western Jurassic, Western Hayfork, Foothills, and related terranes), SA (Santa Ana). Terranes are associated with Farallon subduction include CG—Chugach; FR—Franciscan; PR—Pacific Rim; SC—Siletz-Crescent; VC—Vizcaino.
IMS Superterrane (purple) includes terranes BM (Blue Mountains, CC (Cache Creek), QN (Quesnel), ST (Stikine) and YTT (Yukon Tanana). NJ (Native Jurassic arc) is the onshore continuation of IMS arcs, as is presumably its along-strike continuation of extensional magmatism in Mexico ("Nazas arc"), shown by purple asterisks.

Figure 8. Collisional deformation since ~155 Ma, when NAM first rode into the intra-oceanic MEZ arc, and welded it onto the continent's westward-subducting margin. **(A)** Progression of deformation in three time slices before, during and after suturing. **At 160 Ma**, arc magmatism above the westward-subducting Mezcalera Ocean, at the leading edge of North America (NAM), adds crust to the Insular Superterrane (INS) arc and lithosphere to the MEZ slab wall. Circa 155 Ma, the last of Mezcalera lithosphere is consumed between NAM and easternmost INS: NAM collides with INS microcontinent, resulting in the Nevadan orogeny **At 140 Ma,** deformation at the California margin and upward truncation of the slab wall. As NAM is still being pulled westward (by intact trench segments in and out of the figure plane), subduction polarity at the collided segment is forced to flip. **At 100 Ma,** subduction has flipped, to eastward beneath the margin. Its slab, deposited by subduction of the Southern Farallon plate), creates an

east-dipping blanket (100 Ma panel) as the trench is forced westward in front of advancing NAM. This subduction is building new, margin-hugging arcs that overprint the NAM-INS suture (including the Sierra Nevada batholith). Both north and south of the initial collision site, NAM continues to collide with microcontinental INS, resulting in widening Sevier deformation (Columbian orogeny in Canada).
(B) Generalized cross-section through a continent-beneath-arc suture, such as between NAM and INS. This spatial zoom into the green box in the 140-Ma panel of A is based on a stylized cross section through central Taiwan, a moden example of continent-arc collision with subsequent subduction flip (after Beyssac et al., 2007; section oriented normal to the suture). Both the Taiwan and the INS-NAM sutures show widespread distribution of units containing old detrital zircons, tectonically exhumed forearc (tectonically removed), and high grade, rapidly exhumed metamorphic rocks immediately inboard of the suture. Kmg is Cretaceous orthogneiss (Chipan gneiss) that has cooled through 240 °C in the past million years (Beyssac et al., 2007).

Figure 9. Margin-parallel terrane translations based principally on paleomagnetic data from Late Cretaceous and Eocene strata. These data constrain the tomotectonic terrane reconstruction model of Clennett et al. (2020), which is modified in the figures. (A) Present-day terrane map shows the current locations of a half-dozen units that are very robustly constrained. The green/blue lines, with nodes every 10 Ma and date labels (in Ma) at key times, represent the spatio-temporal trajectories into the past of these units, back to when they were deposited. A 1000-km scale bar is shown for reference. Trajectories are in absolute coordinates relative to the lower mantle, according to our Clennett et al. 2020 reconstruction. This reconstruction honors the displacement constraints of the most solid paleomag sites, Carmacks & Mount Tatlow/Churn Creek, but Spences Bridge is not honored since it does not fully pass the fold test. The model is based on globally derived apparent polar wander paths (APWP), which reach the same conclusion as for APWP derived solely from North American rock units (Housen, 2021; Tikoff et al., 2022). The *main* BajaBC translations are implemented 70-50 Ma along the yellow line, which runs mainly through Intermontane terranes (and their left-behind correlatives in the Blue Mountains/U.S.). This Baja-BC fault line is necessarily speculative, but it must run inboard of all paleomag sites that show significant offsets (details in section 6.2). The trajectory of the Sierra Nevada, illustrative of a non-translated site on stable NAM, is shown in dark green. Accreted superterrane packages follow the colour scheme of Figure 7; additional pericratonic blocks are colored dark and light purple.

(B) Tomotectonic reconstruction of the assembly of Alaska from Baja-BC and Angayucham terrane translations. This 85-Ma snapshot f the Clennett et al. 2020 model reconstructs the configuration of Baja-BC (comprising at a minimum the terranes west of the yellow line) at the onset of its northward sprint. The locations of the Angayucham (red barbs) and northern Farallon trenches (green solid barbs) are constrained by the ANG and CR slabs, respectively. The terranes of the then-active ANG arc (Koyukuk, future Central Alaska, in red) were welded into the Orcas microplate, but gradually being dislodged and rotated by the obliquely colliding NAM – the “Great Alaskan Terrane Wreck” of Johnston (2001). The northern Farallon arc terranes (Pacific Rim, PR, and others now underplating INS) were also intruded into the Orcas plate and slowly accreted against INS. During its northward sprint, Baja-BC effectively became part of the Orcas plate, separated from NAM by the “Baja-BC fault” (yellow line) or collection of faults.
Baja-BC passes *inboard* of, and unimpeded by, the CR Farallon trench, which still sits offshore. As NAM advances westward, Orcas is squeezed out toward the west or north. It may have subducted into one of two small slabs observed under the grey areas (see text). Due to the small size and mobility of the plate, its disappearance can be rapid, and the Baja-BC and Central Alaskan terranes on it are transported along (the “sprint” phase). As the Orcas seafloor subducts, the northern Farallon trench persists and makes landfall on NAM, becoming the continental Cascades arc by ~50 Ma, which shut off this northwestern

passage for shuffling terranes. Baja-BC and Central Alaska collapse against each other and against NAM, completing the assembly of Alaska. The angle between the yellow line (paralleling the NAM margin) and the ANG slab (red line) sets the angle of the Alaskan orocline.